GPR monitoring for road transport infrastructure: A systematic review and machine learning insights

Mezgeen Rasol, Jorge Pais, Vega Pérez-Gracia, Mercedes Solla, Francisco Fernandes, Simona Fontul, David Ayala-Cabrera, Franziska Schmidt, Hossein Assadollahi

▶ **To cite this version:**

Mezgeen Rasol, Jorge Pais, Vega Pérez-Gracia, Mercedes Solla, Francisco Fernandes, et al.. GPR monitoring for road transport infrastructure: A systematic review and machine learning insights. Construction and Building Materials, 2022, 324, pp.126686. 10.1016/j.conbuildmat.2022.126686 . hal-04197350

HAL Id: hal-04197350
https://univ-eiffel.hal.science/hal-04197350v1

Submitted on 11 Jul 2024

HAL is a multi-disciplinary open access archive for the deposit and dissemination of scientific research documents, whether they are published or not. The documents may come from teaching and research institutions in France or abroad, or from public or private research centers.

L'archive ouverte pluridisciplinaire **HAL**, est destinée au dépôt et à la diffusion de documents scientifiques de niveau recherche, publiés ou non, émanant des établissements d'enseignement et de recherche français ou étrangers, des laboratoires publics ou privés.

Investigo
Universidade Vigo

Biblioteca Universitaria
Área de Repositorio Institucional

Tfno.: 986 813 821
investigo@uvigo.gal

Citation for published version:

Mezgeen Rasol, Jorge C. Pais, Vega Pérez-Gracia, Mercedes Solla, Francisco M. Fernandes, Simona Fontul, David Ayala-Cabrera, Franziska Schmidt, Hossein Assadollahi. GPR monitoring for road transport infrastructure: A systematic review and machine learning insights. *Construction and Building Materials*, Volume 324, 2022, 126686, https://doi.org/10.1016/j.conbuildmat.2022.126686

Accepted Manuscript

Link to published version: https://doi.org/10.1016/j.conbuildmat.2022.126686

General rights:

© 2022 Elsevier Ltd. This article is distributed under the terms and conditions of the Creative Commons Attribution-Noncommercial-NoDerivatives (CC BY-NC-ND) licenses.
https://creativecommons.org/licenses/by-nc-nd/4.0/

GPR Monitoring for Road Transport Infrastructure: A Systematic Review and Machine Learning Insights

Mezgeen A. Rasol [1], Jorge C. Pais [2], Vega Pérez-Gracia [3], Mercedes Solla [4], Francisco M. Fernandes [5], Simona Fontul [6], David Ayala-Cabrera[7], Franziska Schmidt[1], Hossein Assadollahi[8]

[1] Université Gustave Eiffel, MAST/EMGCU, 5 Boulevard Descartes, 77454 Marne-la-Vallée cedex 2, France

mezgeen.rasol@univ-eiffel.fr ; franziska.schmidt@univ-eiffel.fr

[2] University of Minho, ISISE, Department of Civil Engineering, Guimarães, Portugal

jpais@civil.uminho.pt

[3] Universidad Politécnica de Cataluña, EEBE School, RMEE Department, Barcelona, Spain

vega.perez@upc.edu

[4] CINTECX, GeoTECH research group, Universidade de Vigo, Vigo, Spain

merchisolla@uvigo.es

[5] University Lusíada – Norte, Largo Tinoco de Sousa, Vila Nova de Famalicão, Portugal

francisco.fernandes@fam.ulusiada.pt

[6] National Laboratory for Civil Engineering (LNEC), Transportation Department, Lisbon, Portugal

simona@lnec.pt

[7] CWRR - School of Civil Engineering, University College Dublin, Belfield, Dublin 4

david.ayala-cabrera@ucd.ie

[8]Setec Group, Structural and Geotechnical Health Monitoring Department, LERM, Paris, France

assadollahi.hossein70@gmail.com;

GPR Monitoring for Road Transport Infrastructure: A Systematic Review and Machine Learning Insights

Mezgeen A. Rasol [1], Jorge C. Pais [2], Vega Pérez-Gracia [3], Mercedes Solla [4], Francisco M. Fernandes [5], Simona Fontul [6], David Ayala-Cabrera[7], Franziska Schmidt[1], Hossein Assadollahi[8]

[1] Université Gustave Eiffel, MAST/EMGCU, 5 Boulevard Descartes, 77454 Marne-la-Vallée cedex 2, France
mezgeen.rasol@univ-eiffel.fr ; franziska.schmidt@univ-eiffel.fr
[2] University of Minho, ISISE, Department of Civil Engineering, Guimarães, Portugal
jpais@civil.uminho.pt
[3] Universidad Politécnica de Cataluña, EEBE School, RMEE Department, Barcelona, Spain
vega.perez@upc.edu
[4] CINTECX, GeoTECH research group, Universidade de Vigo, Vigo, Spain
merchisolla@uvigo.es
[5] University Lusíada – Norte, Largo Tinoco de Sousa, Vila Nova de Famalicão, Portugal
francisco.fernandes@fam.ulusiada.pt
[6] National Laboratory for Civil Engineering (LNEC), Transportation Department, Lisbon, Portugal
simona@lnec.pt
[7] CWRR - School of Civil Engineering, University College Dublin, Belfield, Dublin 4
david.ayala-cabrera@ucd.ie
[8] Setec Group, Structural and Geotechnical Health Monitoring Department, LERM, Paris, France
assadollahi.hossein70@gmail.com;

Abstract

Suitable road pavements assessment becomes essential to provide safe traffic movements of people and goods. Moreover, a reliable transportation network is a crucial aspect of economic growth. Road pavements are subjected to various factors that influence overall performance (e.g., traffic load, temperature, moisture, delamination of the pavement layers, subsurface condition, etc.). These factors can reduce the infrastructure's life and decrease the circulation comfort of the vehicles in the transportation network. Early inspection of pavements optimizes maintenance and repairing methodologies, decreasing the maintenance cost and increasing the lifespan of the road pavements. Non-destructive techniques are strongly recommended to achieve accurate and valuable information from the subsurface condition. Ground Penetrating Radar (GPR) is a non-destructive geophysical method widely used on infrastructure assessment, particularly in road pavements, due to its low operation cost, time-saving, non-invasive, and less workforce. This paper presents a critical state of the art of applying GPR to diagnose road pavement and detect inner damages such as debonding, sinkholes, moisture, etc. The incorporation of the GPR with other complementary techniques in pavement inspection is also discussed. Through the review, the GPR capabilities for road inspection and evaluation of subsurface identification have been successfully demonstrated and validated in numerous studies and case studies. Finally, the application of more

recent processing techniques to support decision-making owners/operators, such as machine learning and intelligent data analysis methods, and the future challenges on the GPR application in road pavements are introduced.

Keywords: GPR, road pavements, NDT, damages, intelligent data analysis, machine learning, inspection, deep learning, decision-making

1. Introduction

1.1 Distresses in road pavement

Throughout the years, highways have been primordial for the mobility of people and goods, despite the increase of different transportation modes, such as transportation by water, rail, and air. The quality and safety of highways transportation depend on their surface regularity and strength offered by road pavements designed to support a given traffic spectrum under certain climatic conditions [1]. Depending on traffic volume and based on a life cycle analysis, pavements can be constructed using asphalt or cement concrete on their surface, which leads to flexible or rigid pavements.

Flexible pavements are composed of granular layers over the pavement foundation and asphalt concrete layers on their top. In contrast, rigid layers are formed by cement concrete layer over a cemented treated base. It is possible to have composite pavements that mix asphalt and cement-based layers providing improved strength due to the cement-based layers and comfort due to the asphalt layers.

Pavement design defines the pavement layers' thickness, which is controlled during and after pavement construction. During construction, spreading equipment and the compaction process ensure that thickness. However, the layer thickness is controlled by probes. After construction, thickness is controlled by holes where it is possible to measure the layer’s thickness or extract cores for further measurement. These verifications only control the pavement thickness punctually. However, continuous control is mandatory to ensure pavement quality. This control can be done using Ground Penetrating Radar (GPR) with good precision after calibration for the layer material. Depending on the layer thickness, different types of equipment should be used, and suitable results have been obtained for very thin asphalt layers [2].

The quality of road materials is related mainly to their density obtained during compaction. Except for certain types of materials, increasing material density increases material quality and extends pavement life. This density can be controlled during and after pavement construction using

equipment for punctual measurement, but a continuous assessment is recommended. This continuous assessment has been made using GPR equipment with exciting results.

The design periods of flexible and rigid pavements are entirely different, but the cracking level characterizes their end-of-life period. Cracking is not the only distress on road pavements. Still, it is the primary indicator for the lack of bearing capacity and thus requires a pavement rehabilitation that, in most cases, is carried out by a pavement overlay. Typically, cracking propagates from the bottom of pavement layers to the top, but in thick pavements, it is often to see cracking that propagates from top to bottom. Cracks are very thin in flexible pavements, but their width increases and can reach 1 or 2 cm due to the traffic and temperature variation. In rigid pavement, cracks are always very thin, but these pavements have joints 1 to 2 cm wide. Even after pavement rehabilitation or reinforcement, existing cracks in the old layers propagate to the new pavement layers. This phenomenon is frequent and is due to the discontinuities in the old pavement layers, and the cracking pattern of the old pavement is reflected in the new layers. In terms of crack width and depth, the cracking condition can be assessed using GPR despite the difficulties inherent to the signal propagation and the crack faces directions. These directions, using ground-coupled antennas, are almost coincident, and measurements are not accessible.

Soils and granular layers have a behaviour influenced by moisture. These materials are compacted for optimum moisture content, and the values above produce a decrease in their bearing capacity. Because bound pavement layers (asphalt or cement-treated layers) are supported by foundation (soil) and granular layer, the missing bearing capacity of these materials (due to the excess of moisture or water) allows the pavement to bend, and the consequent cracking in asphalt and cement-treated layer. Thus, moisture control and its assessment are vital for pavement integrity and have been made using GPR equipment.

The pavement rehabilitation design requires two types of information from the old pavement: the thickness of all layers and their stiffness. The accuracy for stiffness evaluation depends on the exact pavement thickness on the bearing capacity assessment location. Because it is necessary to assess the pavement thickness in all locations where bearing capacity tests are carried out, a continuous evaluation of pavement layers thickness is essential and can be made using GPR measurement. So, a combination of bearing capacity tests and GPR for thickness evaluation is paramount for the correct analysis and design of road pavement and for its rehabilitation.

There are many utilities associated with highways, and the main are the utilities for underground drainage, which must be in good shape for perfect water flow [3]. The main problem of these utilities, when constructed with plastics, is their breaking due to the weight above them. Earth

obstruction is also frequent and avoids proper water flow. The identification and quality state assessment of these utilities is primordial for good underground drainage. Other utilities under highways include electric cables and water pipes, which must be located and identified mainly during highway construction because they are not always well documented. Decision-makers in both transportation agencies and utility companies need timely access to accurate utilities location information to minimize the risk of disruption during highway renewal activities [4].

1.2 GPR background in road pavements

Proper monitoring of road pavement is a challenging task during the lifecycle of road pavements. An appropriate inspection could lead to a better understanding of the current needs and the structural performance status of the road pavements. On the other hand, a comprehensive assessment of road damages provides reliable information to avoid unnecessary economic losses and makes convenient transportation of people and goods available. Road pavement assessment is divided into three main categories: visual inspection, destructive and non-destructive techniques. Visual inspection is usually used when the damage is visible. Road inspection aims to provide valuable but ultimately qualitative information during the initiation stage of damages in road pavements to avoid unnecessary maintenance. Data is obtained from destructive and non-destructive tests. Destructive methods are affected by some aspects: operation time window, cost, professional labour, damage in the pavement's structural elements, and insufficient knowledge of the pavement structure.

For this reason, researchers and road engineers in both academia and industry have strongly recommended the use of non-destructive methods [5], [6]. GPR is a non-destructive geophysical method widely used in the last decades for road pavement subsurface inspection [7]. Thus, GPR has been used in various civil engineering applications, including road pavement assessment and evaluation for repair and maintenance purposes [8]–[15]. The GPR method is based on the propagation of electromagnetic (EM) waves through subsurface media. A transmitter antenna emits pulsed EM signals towards a target medium with a specific wave velocity that depends on the dielectric constant corresponding to each layer. The EM signal is partly reflected at the interface between two different media and returns to the receiver antenna, and partly transmitted into deeper layers until it reaches the time window established in setting parameters (Figure 1) [16], [17]. The reflected wave is based on the amplitude strength, proportionally dependent on the dielectric constant for each subsurface layer. The larger the dielectric contrast, the higher the reflection amplitude is. EM wave velocity depends on the centre frequency of the GPR antenna and subsurface conditions. For instance, higher wave velocity is achieved in dry than wet conditions [18].

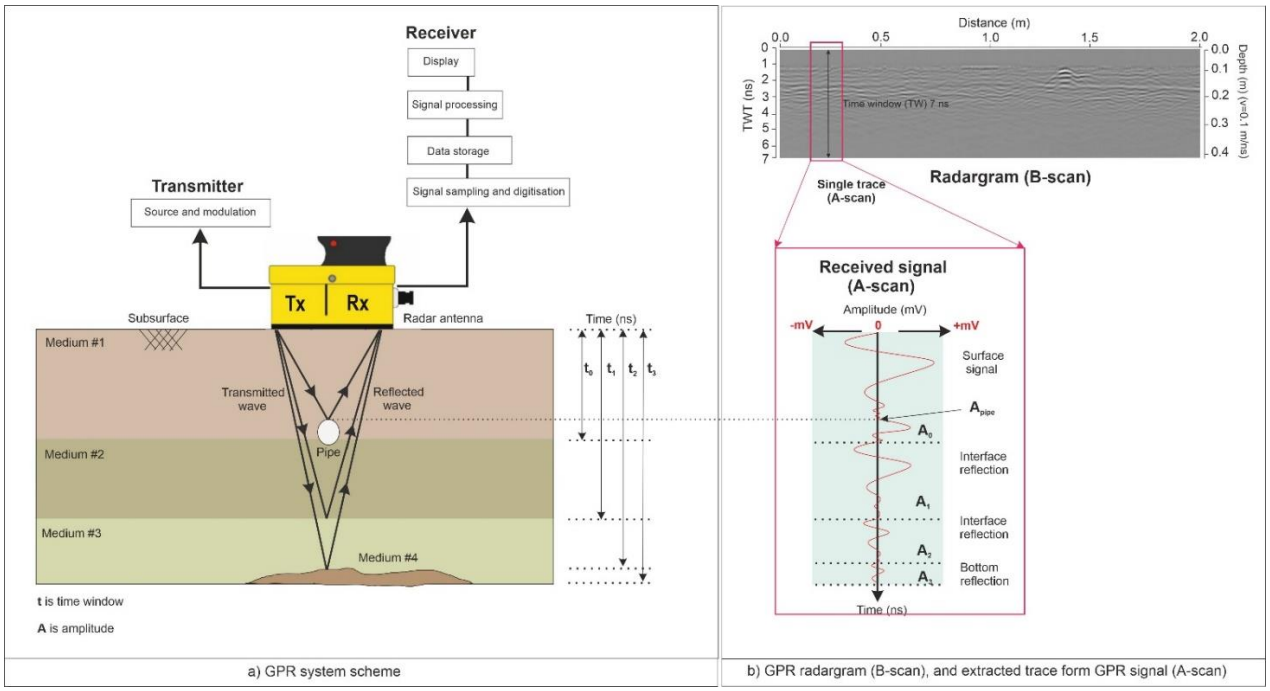

Figure 1 a) Scheme of a GPR system, b) visualization of an A-scan and a B-scan (adapted from [16]).

1.3 Advantages and limitations of current GPR technique

The GPR method is considered one of the most flexible and versatile non-invasive geophysical techniques, which has many advantages for road pavement inspection work and civil engineering applications [7], [16] Alongside the main strengths of the GPR method, various limitations are observed in previous studies and research works. Table 1 presents a list of advantages and limitations of the current GPR technique for road pavements inspection.

Table 1 List of possible advantages and limitations of the current GPR technique.

No.	Advantages	Limitations
1	High speed of inspection operation	High conductivity of materials such as clay and saturated clay
2	Mobile data acquisition or clouding sources	Signal attenuation in heterogeneous subsurface conditions
3	Low cost of the inspection operation	Scattering and backscattering of GPR signal
4	Less labour professional	Expert knowledge to process/interprets radar images
5	In-service road transports during the inspection	Depth of penetration highly dependent on the centre frequency of antenna and ground material condition

1.4 Objectives

This paper presents a critical review and progress of road transport monitoring opportunities by using GPR equipments, including the main applications related to road pavements. One of the main sections of this paper address current challenges, methodologies of the complex data analysis based on machine learning and other possible complex data analysis approaches. An advanced intelligent data analysis leads to a better understanding of road pavements and potential damages, which can be valuable information for repairing and maintenance processes. This analysis can be

an efficient approach to provide a helpful tool for owners/operators to monitor road pavements, obtain a green sustainable transport infrastructure, and overcome the current challenges and constraints in road pavement inspection. Moreover, through the literature review of this paper, some current methodologies are presented in terms of best practices of machine learning, intelligent data analysis of complex radar images, and recent advances in the field aiming to improve the application of GPR and avoid misinterpretation of radar images. Besides, a few European projects are presented in the area of advanced robotic platforms for road transports. The framework for systematic review of our research study is illustrated in Figure 2. This review study upgrades the current knowledge, literature by comprehensively reviewing the main distresses and features are occurs as a real damages over time on-site, and the possibility of the use of machine learning apparoaches to enhance the radar images, and this work is dedicated to present different ML approaches which can be efficient for the road pavement monitoring as a complementary approaches in order to provide better interprobility of radar images.

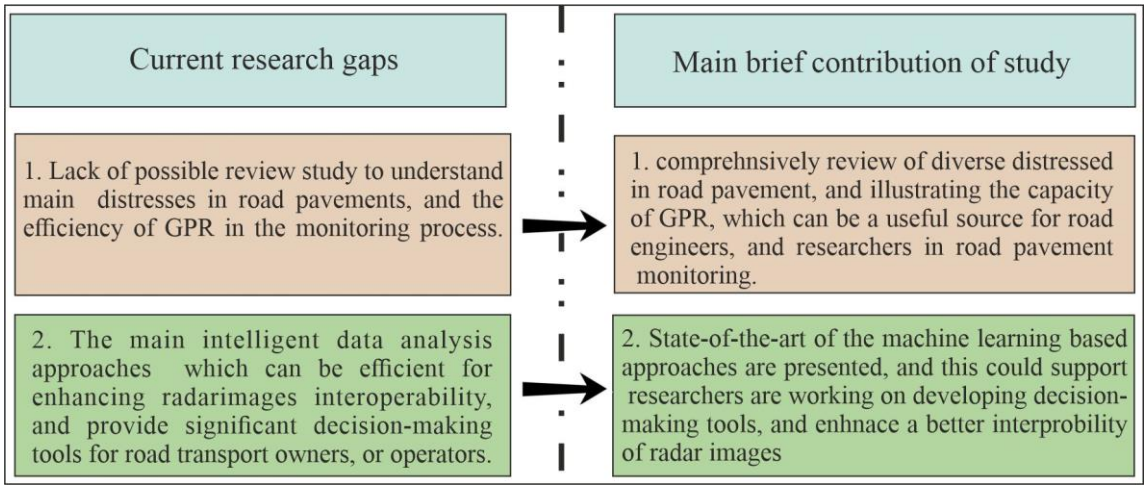

Figure 2 Existing research gaps vs main brief contrbution of this review study.

1.5 Review Methodology

This paper highlights the main current progress and monitoring opportunities for road pavement inspection. The information considered in this review includes the main challenges addressed by the industry and researchers during the last two decades. The analysis is divided into three parts:

i) those studies corresponding to the road pavement structure (i.e., layer thickness, thin-layer thickness, delamination and compaction of pavement layers, and conductivity properties of materials);

ii) those studies dealing with the subsurface conditions of road pavement such as inner damages and deteriorations that occur along the road pavement lifecycle (i.e., cracking, delamination/debonding of pavement layers, subsidence and sinkholes, moisture content of granular and subgrade layer, etc.);

iii) underground utilities in the subsurface of road pavements.

The following criteria were considered in this review:

- More than 100 studies over 20 years in GPR application on road pavements;
- Two main categories of the road pavements are considered, i.e., flexible and rigid pavements;
- Pavement surface and subsurface distresses and real scale damages;
- Intelligent data analysis approaches based on machine learning and deep learning are presented;
- New trends, research projects and future directions are also presented.

2. GPR application on road pavement structure

Road pavements use several types of equipment for assessment during construction, in service, and after rehabilitation. Physical properties are obtained with these equipments to support the design, maintenance, and rehabilitation of road pavements. GPR application on road pavements dates back to the 1990s [19], [20], when a GPR was developed and used in various civil engineering applications, in this case for inspection of the pavement condition to provide a preventive maintenance plan. Significant applications have been made to measure pavement layer thickness and density, which are supported by assessing the dielectric permittivity of road materials. This chapter focuses on these applications.

2.1 Layer thickness measurement

Assessment and management of roads require layer thickness control. This information is crucial in quality control and for the evaluation of their remaining service life. Non-destructive tests (NDT) with GPR have been proved a helpful procedure that provides precise information for pavement maintenance and rehabilitation design. Therefore, this technique is nowadays fully applied as the primary or complimentary test method in regular road inspections, which is usually combined with Falling Weight Deflectometer (FWD) and coring. NDT applications reduce the number of invasive tests, the conventional approach that consisted of extracting pavement cores.

Many authors have described the methodology applied in GPR assessments, demonstrating the accuracy for:

- pavements composed of thick layers [2];
- acquiring data with a common offset and with common midpoint procedure [21];
- developing methods to detect automatically multiple layers, arriving at errors of about 2.5% [22].

The method has been included in guides for pavement evaluation in several countries. For example, the guide [23] contains the procedures recommended in the GPR inspection of bituminous and concrete pavements to assess thicknesses of layers. The standard alert about two problematic scenarios at which assessment can be difficult or even impossible: saturated pavements and extreme iron content in the aggregates. In these two cases, penetration depth could be insufficient to evaluate the state of the pavement because of the high signal attenuation. The use of GPR in roads evaluation has also been included in recommendations developed in different countries. This is the case of the Belgian [24] and British [25] regulations and the Mara Nord Project [26], a project developed in cooperation between the Nordic road administrations.

In most cases, thickness data is obtained from common offset measurements with impulse radar systems, usually with air-coupled antennas [27]. Those antennas are placed on a vehicle, suspended at a height of about 50 cm from the pavement surface. Data is acquired at a regular traffic speed, without impact on the use of the road, and pulses are emitted each 20 to 50 cm. Despite their low penetration and the distance between measurement points, their speed in data acquisition makes them ideal for the study of pavement layer thicknesses. However, in the case of more detailed studies of higher penetration depth required, the analysis is usually carried out with ground-coupled antennas. In this case, the antennas are in contact with the ground, being the data acquisition speed lower than in the case of air-coupled antennas, but reaching greater depths of study, which allows the analysis of the contact between the pavement and the ground, or the detection of anomalous targets under the pavement. Figure 3 presents an example of the image obtained with a 500 MHz centre frequency ground-coupled antenna during the study of the pavement of a main street in a dense city.

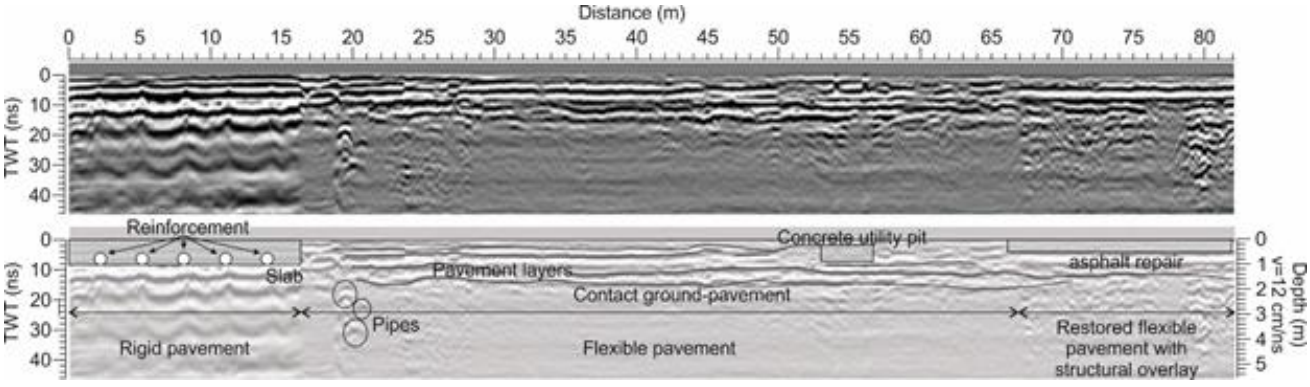

Figure 3. Radar image of pavement layers. The discontinuities are associated with the contacts between layers. The presence of other targets is also detected.

In Figure 3 it is possible to distinguish between three different parts of the road: a concrete pavement (at the beginning of the profile), a flexible pavement (in the central part of the image) and, at the end of the profile, a flexible repaired pavement. In the three parts, the layers are

detected, combined with other anomalies corresponding to reinforcement or utilities. However, the images obtained in the flexible pavement are more detailed than those obtained in the other parts of the road. The contact between the subbase and the ground is clearly identified only in this part. The analysis of thickness layers is more difficult in the case of deteriorated material, older pavements or repaired roads.

The use of antennas arrays has also been evaluated and tested in different sites and laboratories, obtaining errors under 10% in the thickness estimation [28]. Many authors recommend using higher frequency antennas combined with lower frequency antennas to obtain an effective balance between resolution of the shallowest layers and penetration depth to detect the contact with the ground of anomalies placed under the pavement [29]. However, the conclusion of many analyses indicates that the thickness estimation accuracy in the case of non-uniform thickness layers is less than in the case of uniform layers. The precision depends on the calibration of the antennas [30] and on the approaches to assign dielectric constants to each pavement layer. The analysis presented by [31] compares three approaches that allow determining the dielectric constant of the layers: a direct estimation from GPR data, comparing GPR data with cores and, finally, using laboratory tests. The first method, which is using direct esti;ation from GPR datais the most imprecise, but it is as effective as a quick and rough procedure, compared with cores, this is one of the most effective methods, and non-invasive to detect the thickness layer then compared with core samples. The inconvenient is that in order to increase the accuracy requires a large number of cores, or in some cases an advance data analysis is a key to increase a better accuracy for the purpose of the decision-making assessment.

The detection of layer thickness (h) based on the estimated dielectric permittivity (ε_r) of each layer starts with the detection of the echoes time (t) and the analysis of the wave velocity (v) or dielectric permittivity at each layer, as indicated in Equation 1:

$$h = \frac{vt}{2} = \frac{c\,t}{2\sqrt{\varepsilon_r}} \qquad \text{Equation 1}$$

The direct estimation of the wave velocity from the GPR data usually is based on comparing the amplitudes of the different echoes, being the dielectric permittivity of the layer n, ε_{rn}:

$$\varepsilon_{rn} = \varepsilon_{r(n-1)} \left\{ \frac{1 - \left(\frac{A_0}{A_{inc}}\right)^2 - \sum_{i=1}^{n-2} Ri \left(\frac{A_i}{A_{inc}}\right) - \left(\frac{A_{n-1}}{A_{inc}}\right)}{1 - \left(\frac{A_0}{A_{inc}}\right)^2 - \sum_{i=1}^{n-2} Ri \left(\frac{A_i}{A_{inc}}\right) + \left(\frac{A_{n-1}}{A_{inc}}\right)} \right\}^2 \qquad \text{Equation 2}$$

Being ε_{rn}, $\varepsilon_{r(n-1)}$ the dielectric permittivity at layers n and $n-1$, A_o the amplitude of the echo from the first discontinuity, A_{inc} is the amplitude of the incident signal, A_i is the amplitude of the echo from the $i+1$ discontinuity, and R_i is the reflection coefficient from the i discontinuity.On the other hand,

several factors are affecting the detection of pavement thickness layer results, mainly, subsurface condition, antenna frequency, noisy data, lack of information, combination of GPR signal between different layers and ground size distbution of the media properties. Beside that the use of an appropriate data processing is essential, for example using full-wave inversion, or using straight ray methods for layer thickness or thin layer thickness [32]. In the following section more details are presented for the thin-layer thickness assessment.

2.2 Thin-layer thickness assessment

Although layer thickness identification is one of the most typical GPR applications in pavements, the depth and thick resolution are lower in thinner layers, having the highest difficulty in detecting and separating the first echoes. Thin layers are those layers whose thickness is about the wavelength of the incident wave. The echoes from both surfaces of a thin layer are detected as overlapped anomalies in the GPR data, being difficult to distinguish the time of the arrivals. Therefore, the usual evaluation of the images, using raw data or simple processing, is useless to determine the layer thickness. The identification of close reflective surfaces depends on the GPR vertical resolution, which theoretically is considered.

However, in field surveys, the vertical resolution is approximately the wavelength [33]. Although this limit, GPR is sensitive to the existence of those thin layers. The resultant waveform of the signal reflected on the top and bottom surfaces includes the coupling effects of both reflections, and the shape and length differ from the source pulse. Based on those reflective properties, [34] defined a thin layer as the layer whose thickness is less or equal to the predominant wavelength divided by 8, obtaining the wavelength from the frequencies of the wave and the propagation velocity in the layer material.

Thin layers are those layers with a thickness similar or smaller to the wavelength. Distinguishing between the reflections on the top and the bottom of the layer is difficult or even impossible.

The accurate estimation of layer thickness requires a precise determination of the two-way travel time of each reflection, which is not possible in the case of layers with thin thickness compared with the electromagnetic incident wave length. The superposition of different reflections makes it difficult or even impossible to determine those times. Consequently, noticeable errors affect the estimation of the dielectric permittivities, leading to an inaccurate estimation of the thickness.

The problem of thin layers analysis has been evaluated by different authors. [35] analysed the thickness estimation using GPR based on the vertical resolution of each antenna and distinguished between rigid and flexible pavements. The work observes the difficulty in separate reflections due to the overlap of waves. It also concluded that, in most cases, the estimated thickness is an average

value that combines several layers, detected as a single one. The different dielectric permittivity from thin layers produces an overestimation of the total thickness. Determining the correct average wave velocity inside the layers group and deconvolution in the data processing could produce more accurate results. [36] proposed the regularized deconvolution to increase the thin layer detection accuracy. They concluded that the error is less than the construction tolerance but only in the case of a previous calibration. The analysis carried out by [35] compared the errors without calibration for thick layers (more than 50 mm thick) with intermediate layers (between 30 mm and 40 mm thick) and thin layers (between 25 mm and 19 mm thick), obtaining errors lesser than 8%. Still, for thin layers, the errors present a wide variation, about 55%. The work demonstrates that the error reduces dramatically when a core is used to calibrate the dielectric constant of each layer.

[37] analysed thin layer asphalt concrete (thickness between 19 and 50 mm) during compaction, obtaining similar errors in the thickness estimation. Errors between 8% and 10% are obtained in field surveys, while errors of about 9% and 1% affect the simulation results. The thickness of this asphalt concrete layer is also analysed by [38] using a nonlinear gradient descent method. This method produces accurate results but requires knowledge of the pavement structure.

High-frequency antennas between 1 and 2 GHz are recommended to improve the vertical resolution and processing techniques to improve the time resolution [39], combined with numerical models [37]. The technic and results depend highly on the signal-to-noise ratio in the radargrams. Studies in sediments demonstrated that the data spectrum is sensible to the existence of thin layers. These elements produce a shift towards high frequencies [40]. Applications of spectra analysis in pavement assessment demonstrates the sensibility of spectrum in layers of about 12 cm, using a 900 MHz centre frequency antenna [41] , presenting changes in the amplitude corresponding to the different layers' materials. In addition, the amplitude of the spectrum is reduced, and the peaks move to lower frequencies when thickness increases [42].

However, [22] concluded that the thickness estimation of thin layers is still a complex problem due to the vertical resolution of the antennas; although accurate results have been obtained in the case of the thin top layer thickness, using high pass filter and trace correlations [27]; or using a regularized deconvolution algorithm that allows to distinguish between overlapped signals, improving the vertical resolution in the radargrams [35] . Another proposed solution refers to the design of new equipment and antennas. An example is the proposal described by [43], a step-frequency radar operating in a range of 500 MHz to 6 GHz, specially designed for pavement assessment. The tests in controlled areas indicate that this equipment can detect shallow layers of about 2.5 cm.

2.3 Dielectric permittivity of road materials

The dielectric permittivity (ε) is an essential quantity for GPR measurements. The terms relative permittivity (k) or dielectric constant are often used and defined in Equation 3, where ε_0 is the permittivity of vacuum, 8.89×10^{-12} F/m.

$$k = \frac{\varepsilon}{\varepsilon_0} \qquad \text{Equation 3}$$

Road pavements have four materials, namely asphalt mixtures, cement concrete, granular materials, and soils. These materials are composed of elementary components such as asphalt, aggregates, air, cement, water, and solid particles, as represented in Figure . The dielectric permittivity of the bulk material is function of the percentage and dielectric permittivity of their components. Road materials typically have a dielectric permittivity in the range of 3-8.

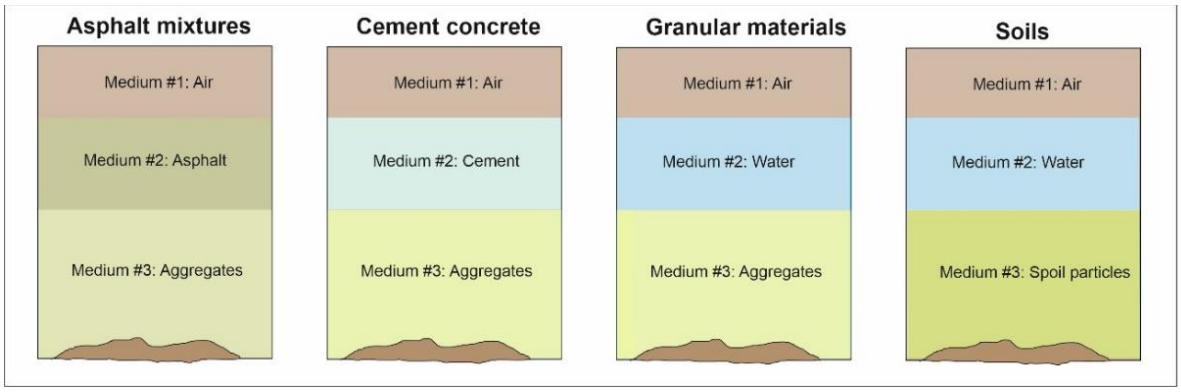

Figure 4. Schematic representation of road pavement materials showing their components (not to scale).

Based on the CRIM, the dielectric constant can be estimated by Equation 4 [44] for the case of an asphalt mixture,

$$(\varepsilon_{am})^{\frac{1}{\alpha}} = \theta_{ag}(\varepsilon_{ag})^{\frac{1}{\alpha}} + \theta_{ap}(\varepsilon_{ap})^{\frac{1}{\alpha}} + \theta_v(\varepsilon_v)^{\frac{1}{\alpha}} \qquad \text{Equation 43}$$

where:

ε_{am} = dielectric constant of the asphalt mix;

α = parameter dependent on the mix composition (usually assumed to be 2);

θ_{ag}, θ_{ap}, θ_v = volumetric concentrations of aggregate, asphalt and air-voids, respectively;

ε_{ag}, ε_{ap}, ε_v = dielectric constants of the aggregate (typically 4 to 8), asphalt (typically 2 to 4) and air (1), respectively.

Considering the dielectric constants of the air and $\alpha = 2$, Equation 4 can therefore be simplified as expressed in Equation 5.

$$\sqrt{\varepsilon_{am}} = \theta_{ag}\sqrt{\varepsilon_{ag}} + \theta_{ap}\sqrt{\varepsilon_{ap}} + \theta_v \qquad \text{Equation 5}$$

This model can be used for the other road materials with suitable changes due to different components, mainly water for granular materials and soils.

A correct calculation of the dielectric permittivity is essential for GPR data processing as it is necessary for all measurements in road pavements. Usually, dielectric permittivity is calculated by a back-calculation procedure by reference materials when using ground-coupled systems. However, for air-coupled antenna systems, the surface reflection method is the most used. It is based on comparing the reflection amplitude from the pavement and the metal plate reflection.

Equation 6 presents the model for the dielectric permittivity of the asphalt layer of road pavements,

$$\varepsilon_1 = \left(\frac{1+\frac{A_1}{A_m}}{1-\frac{A_1}{A_m}}\right)^2 \quad \text{Equation 6}$$

where

ε_1 = dielectric permittivity of the asphalt layer;

A_1= amplitude of the reflection from the top of the pavement;

A_m= amplitude of the reflection from a metal plate.

For the granular layer (second layer) of asphalt pavements, dielectric permittivity is calculated as indicated in Equation 7,

$$\sqrt{\varepsilon_2} = \sqrt{\varepsilon_1}\left[\frac{1-\left(\frac{A_1}{A_m}\right)^2+\left(\frac{A_2}{A_m}\right)}{1-\left(\frac{A_1}{A_m}\right)-\left(\frac{A_2}{A_m}\right)}\right] \quad \text{Equation 7}$$

where

ε_2 = dielectric permittivity of the granular layer (second layer);

A_2= amplitude of the reflection from the top of the granular layer.

Recently [45] developed an innovative method for measuring pavement dielectric constant using the extended common mid-point method with two air-coupled GPR systems. This method works better for pavements with non-uniform thickness than the classic method based on surface reflection. Also, the technique dispenses the use of a ground-coupled antenna. Therefore, the time delays of the two GPR systems can be estimated at a higher level of accuracy, and the GPR survey can be conducted at a higher speed. They obtained dielectric constants for the asphalt layer ranging between 5.3 and 8.4 in a trial section with four different thicknesses.

An attempt was made by [28] to measure dielectric permittivity using an antenna array GPR. The antenna was calibrated considering the phase centre and the antenna offset, which improved the velocity and thickness estimations accuracy compared with the conventional method.

[46] proposed a methodology for determining the dielectric permittivity of soils using the Born Approximation and demonstrated that the electrical field scattered by a spot-like buried object permits accurate estimation of the soil permittivity even when no information of the soil conductivity is available. In above-mentioned previous studies it is strongly recommended to calibrate GPR antenna before using in the expriemental campagain to avoid or minimize errors of calculating dilerctric constant. Besides, there are several factors can influence of the clarity of the dielectric constant, mainly are vertical and horizontal resolution based on antenna frequency and subsurface conditions, wet or moisture condition, external signals which mislead the gpr signal, attenuation of GPR signal, and during the postprocessing it is also essential to select an appropriate set of filters in order to maintain the correct dielectric constant.

2.4 Density/compaction of asphalt layers

The density of bituminous concrete layers is highly dependent on its constituents, especially the percentage of bitumen and the compaction energy. The density can be assessed by calculating the dielectric constant of the bituminous layers and using the Complex Refractive Index Model (CRIM) theory [44]. CRIM is used to estimate the permittivity of heterogeneous mixtures based on their single components and pavement geometry. This equation has been used to calculate the density of the asphalt mixes by knowing the volumetric characteristics of the asphalt mixes, in terms of asphalt and air-void content, as a function of the dielectric constant of the aggregates and asphalt. Due to its simplicity, it is widely applied for GPR applications because GPR allows the assessment of the parameters necessary to use CRIM, such as dielectric constants and geometry.

Considering the data obtained from GPR, it is possible to use the CRIM model to get information about the bulk specific gravity (or apparent density) of asphalt mixtures. The correlation between asphalt mixtures apparent density (G_{mb}), dielectric values of the individual components (binder, ε_{mb}, and aggregates, ε_s), specific gravity (relative density) of binder (G_b) and asphalt mixtures (G_{mm}), the apparent density of aggregate (G_{sb}) and binder content (P_b) is given by Equation 8.

$$G_{mb} = \frac{\sqrt{\varepsilon_{HMA}}-1}{\frac{P_b}{G_b}\sqrt{\varepsilon_b}+\frac{(1-P_b)}{G_{sb}}\sqrt{\varepsilon_s}-\frac{1}{G_{mm}}} \quad \text{Equation 8}$$

Other authors produce other models, namely the Rayleigh and the Böttcher Mixing Models. Both allow estimating the asphalt mixtures density from known or measured values with GPR. The respective Equations 9 and 10 are as follows:

$$G_{mb} = \frac{\frac{\varepsilon_{HMA}-\varepsilon_b}{\varepsilon_{HMA}+2\varepsilon_b} - \frac{1-\varepsilon_b}{1+2\varepsilon_b}}{\left(\frac{\varepsilon_s-\varepsilon_b}{\varepsilon_s+2\varepsilon_b}\right)\left(\frac{1-P_b}{G_{sb}}\right) - \left(\frac{1-\varepsilon_b}{1+2\varepsilon_b}\right)\left(\frac{1}{G_{mm}}\right)} \quad \text{Rayleigh Mixing Model} \quad \text{Equation 9}$$

$$G_{mb} = \frac{\frac{\varepsilon_{HMA}-\varepsilon_b}{3\varepsilon_{HMA}} - \frac{1-\varepsilon_b}{1+2\varepsilon_b}}{\left(\frac{\varepsilon_s-\varepsilon_b}{\varepsilon_s+2\varepsilon_b}\right)\left(\frac{1-P_b}{G_{sb}}\right) - \left(\frac{1-\varepsilon_b}{1+2\varepsilon_b}\right)\left(\frac{1}{G_{mm}}\right)} \quad \text{Böttcher Mixing Model} \quad \text{Equation 10}$$

These models produce similar results in predicting the density of asphalt mixtures based on the dielectric constant and percentages of constituents. Based on this model, the density of the asphalt layer increases with dielectric values. It was found that dielectric values also correlate with the percentage of bitumen, which results in the density increasing with the percentage of bitumen. In a recent study by Fernandes and Pais [5], a laboratory program was established to check the GPR's capability in detecting the value of the asphalt mixtures apparent density in pavements with different densities and different water saturation levels. In this study, six small slabs were produced varying air-void content and bitumen content. GPR measurements using a high-frequency antenna (1.6 GHz) were performed on all slabs without water, and the dielectric constant of the asphalt mixtures layer was obtained. In Figure 5 (left), the asphalt mixtures apparent density using the CRIM increases with the increase in dielectrics, increasing the bitumen percentage. This fact is expected considering that more binder, less voids, thus, slightly higher dielectric value. Figure 5(right) shows an increase in the dielectric value with the percentage of bitumen and the maximum specific gravity of asphalt mixtures.

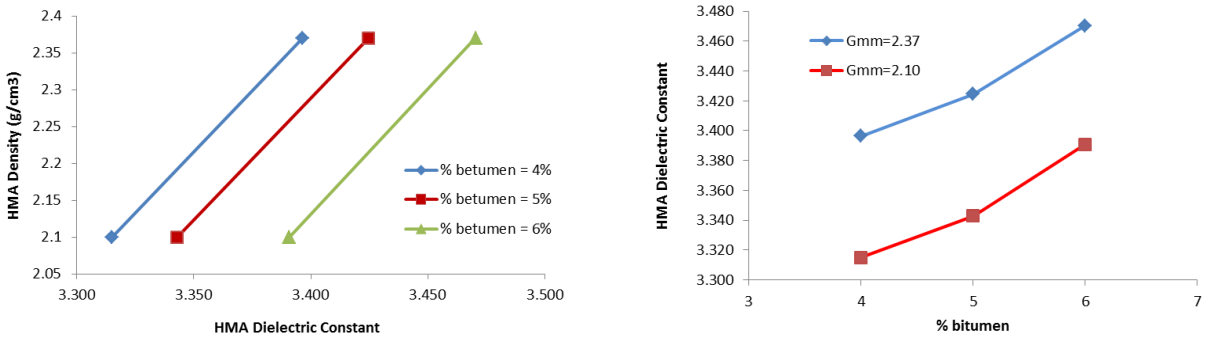

Figure 5. Correlation between density, dielectric constant, percentage of bitumen and maximum specific gravity of asphalt mixtures.

3. GPR Application of Road Pavement Subsurface conditions

GPR has also been used for assessing subsurface pavement conditions and all utilities below the pavement. Thus, this chapter focus on the characterization of cracks existing in rehabilitated concrete pavements, the evaluation of the delamination/debonding of asphalt layers, the detection of subsidence and sinkholes, the assessment of moisture in granular and subgrade layers, and finally on the identification of utilities, mainly drainage pipes. Some examples of these applications and the relevant studies will be presented.

3.1 Cracking identification

Cracking is one of the most common problems in the road pavement, which occurs due to the severe deformation and deterioration in road pavements. Cracks are caused by some factors, namely, the passage of heavy load trucks, pavement ageing, pavement mixture materials (e.g., shrinkage and expansion of the pavement materials), natural hazards and subgrade properties (e.g., landslides, liquefications, and settlements), weather conditions and climacteric agents (e.g., temperature, icing, water film thickness, snow and rain) [6], [13], [47], [48]. Crack dimension (width and depth) generates different effects on road pavement serviceability. Cracks are usually one of the leading causes that could significantly influence the structural performance of the road pavement. Crack inspection is essential in road pavements. Regular repairs and maintenance can prevent any uncontrolled hazards to increase the life cycle of road pavement. These repairs are supported by an appropriate observation strategy in road conditions. Non-invasive techniques such as GPR are widely recommended to provide valuable information about road pavement conditions [16]. A high-resolution 2300 MHz GPR shielded antenna has been applied to identify cracking patterns and early cracks in composite road pavements composed of two layers (asphalt layer over a concrete layer) [49]. Figure 6 shows a GPR survey conducted in a composite pavement to identify surface cracks and internal cracks before propagating to the pavement surface. The processed radar image shows the road structure and various features (e.g., steel rebars, cracks in the asphalt and concrete layer, superficial cracks, and geogrid).

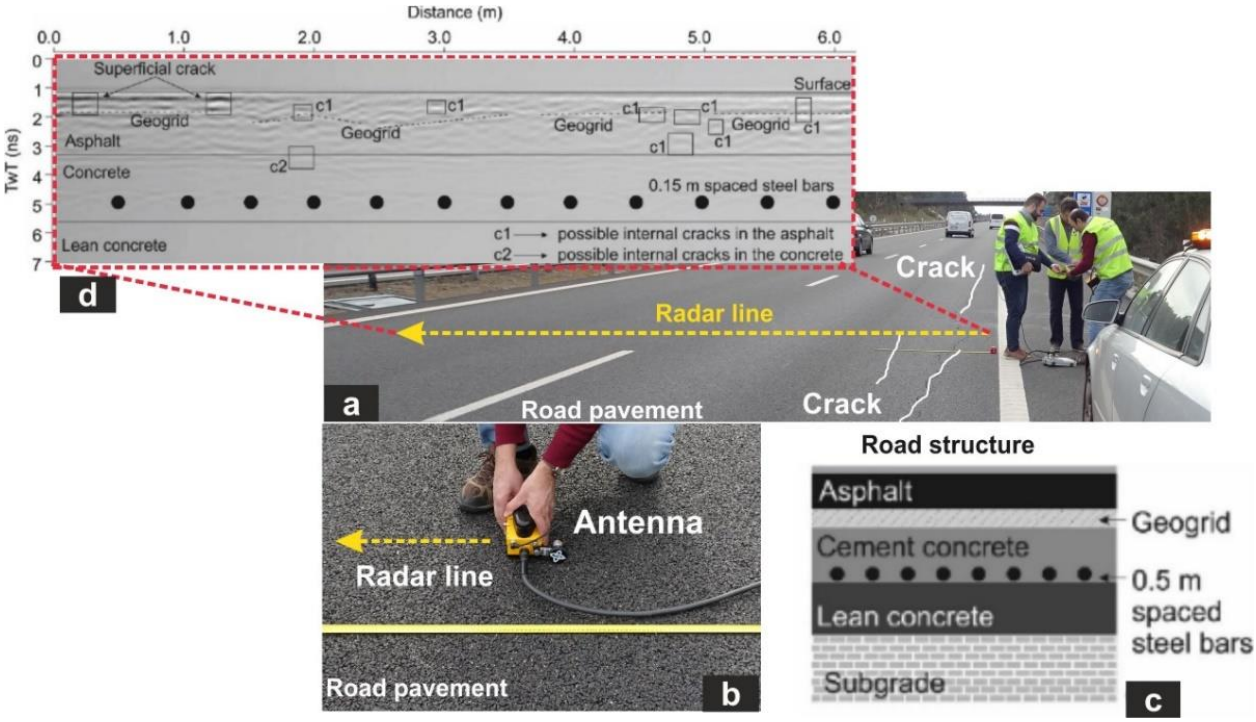

Figure 6 GPR survey on an asphalt pavement adapted from [13]: (a) view of the highway, (b) 2.3 GHz GPR antenna applied on the road section, (c) road structure composed in different layers, (d) processed radar image.

GPR has been extensively underlined in many road pavements research studies in academia and industry during the last 30 years. Cracking is commonly studied in critical road infrastructures, and different features and causes have been investigated. Table 2 presents detailed information, crack dimensions, GPR antenna and supplementary analysis of road pavement studies in previous works.

Table 2 Cracking inspection previous studies and methodologies considered during these works, and each study is referred to its original references.

No.	Cracking condition	Antenna (MHz)	Antenna dipole orientation	Depth (mm)	Width (mm)	Extra features	Pavement type	Crack observation	GPR signal analysis	Numerical modelling	References
1	Vertical cracks	250 and 1000	Perpendicular to the crack line	(45-350)	(1-5)	-Granular layer	Asphalt	Detected	Amplitude	2D and 3D FDTD[1]	[47]
2	Early cracking	2300	Perpendicular and parallel to the crack line	(100-200)	(10 - 20)	-Steel rebars -Settlement in steel rebars -Lean concrete layer	Concrete layer covered by asphalt layer	Detected	Amplitude	2D FDTD[1]	[6]
3	Cracks	1600	Perpendicular and parallel to the crack line	150	(2-30)	Dielectric constant	Cement concrete	Detected	Amplitude	2D FDTD[1]	[49]
4	Cracks	1600	Perpendicular and parallel to the crack line	150	(2-30)	-Dielectric constant -Weather condition and filed cracks with air, sand, water, saturated sand and bitumen -Early cracks - Surface cracks -steel rebars	Cement concrete	Detected	Amplitude	2D FDTD[1]	[13]
5	Cracks	1000	Perpendicular to the crack line	10-28	3	- temperature -water content	Asphalt	Detected	-Amplitude analysis considering width of cracks - Thermograms	2D FDTD[1]	[50]
6	Layer thickness and cracks	800 and 950	-	-	30	- porosity -moisture -layer thickness	Asphalt	-	-Amplitude -Frequency	None	[51]
7	Transversal cracks	2200	Perpendicular and parallel to the crack line	-	Small size	Pavement structure	Asphalt	Detected	-Amplitude -Core samples	None	[52]
8	Vertical and horizontal cracks	250 and 800	Perpendicular to the crack line (simulated data)	5	5	Rock in pavement	Concrete	Detected	-F-K Migration -2D wavelet analysis	None	[53]

FDTD[1] Finite-difference time-domain method is a common numerical analysis of computational electromagnetic waves (http://www.gprmax.com/).

3.2 Delamination/debonding of pavement layers

Debonding of pavement layers affects the bearing capacity of the pavement. The bounding condition between asphalt layers is a significant feature to be considered during the pavement structural evaluation. The significance is because the commonly used numerical models for flexible pavement are linear elastic, and erroneous results can be obtained for layer moduli if the debonding condition between layers is not considered [54]. In addition, water can infiltrate between layers and accelerate the deterioration of the asphalt interface. Debonding can appear during the construction stage due to dirty surfaces, inadequate tack coating, or pavement operation. Antireflective cracking solutions, such as geosynthetics, geotextiles or geogrids, applied for pavement reinforcement, can also cause debonding. Detection of the debonding between layers is a challenge considering only traditional techniques. In the past, coring samples (pits) were considered the most efficient method to diagnose the debonding condition. Nevertheless, layers can debond even more during the extraction of coring samples, which is considered a limitation of the coring tests, and results can be erroneous. Detection of the debonding condition is essential to adequately provide comprehensive information related to the layers for rehabilitation purposes. This detection will support a proper plan for overlaying solutions that mitigate the debonding, such as milling and overlaying. On the other hand, a few different techniques can also be used to observe the bonding condition, such as FWD. A case study of using FWD for debonding condition inspection is presented in Figure 7 in which, between 800 m and 1400 m the difference between the highest deflection (D0) and the second-highest (D1) is observed, which is the detection area of the debonding compared to the rest layers of the pavement [54].

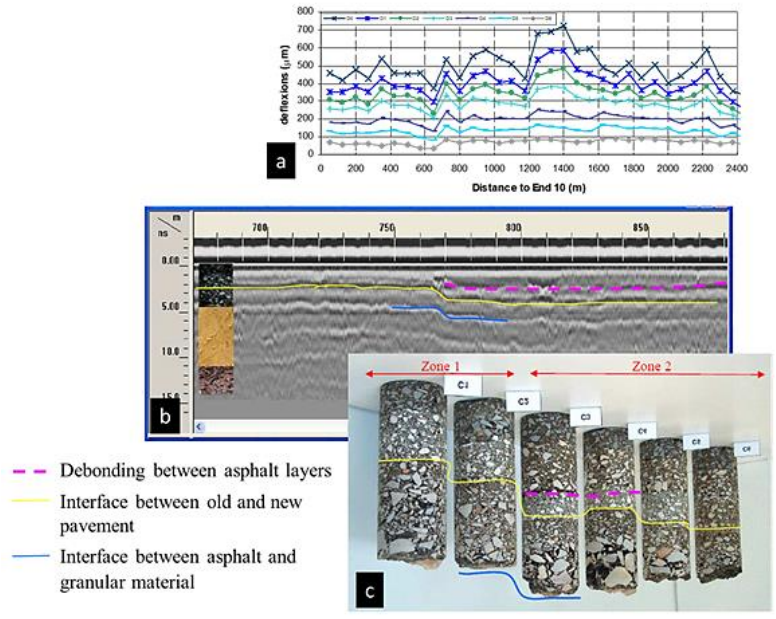

Figure 7 NDT combined survey of an airfield pavement with the identification of asphalt layer interfaces and debonding section - adapted from [54] (a) FWD spectrum, (b) GPR B-scan at the transition between zone 1 and 2 (using 1.0 GHz air-coupled horn antenna) and (c) cores extracted along the pavement.

A research program was dedicated to the study of delamination detection using NDT. Each NDT technology measurement is based on scientific principles related to the measured response from the material properties. Theoretical modelling is commonly used to predict the response for debonding and stripping in the asphalt pavements. The main aim of the modelling is to demonstrate the theory response of each test and the main aspects of the key measurements of the road pavement. For example, the FWD model is also used for back-calculation for FWD test data. Results show that the amount of deflection in pavement changes as the depth of delamination changes considering the non-linear relationship [55]. In the mentioned study, various NDT methods were studied, such as GPR (antenna array, frequency sweep), mechanical wave technology (impact echo (IE) and spectral analysis of surface waves (SASW)). GPR technology has proven to be the most efficient NDT technology capable of testing full lane width at a moderate testing speed (60 km/h).

On the other hand, other NDT methods such as the mechanical wave technique significantly have less testing operation time but are limited at a speed of less than (8 km/h). The main conclusions from this work prove that the GPR can identify variations in the pavement, isolate the depth of a discontinuity in the pavement, and provide a relative degree of severity. Detecting debonding between asphalt layers is possible with the current analysis methodology, and only when moisture is trapped in the debonded area between the layers. None of the NDT technologies can identify partial debonding due to inadequate tack coat during construction. It is highlighted that GPR, IE, and SASW can be valuable project-level tools. A specific data analysis is required to allow NDT into a network-level tool for detecting delamination in asphalt pavements.

Several studies were carried out in the Nantes Accelerated Pavement Testing facility to thoroughly study the behaviour of debonding pavements and the possibility of GPR detecting debonding [56]–[58]. In these researches, advanced post-processing methods were also implemented for data interpretation, such as support vector machines (SVM) [56]. The main tasks were the detection of the horizontal debonding occurring between the first two pavement layers from Stepped-frequency Radar (SFR) [56] data and air-coupled ultra-wideband GPR antennas (SF-GPR), two wideband 2D ground-coupled GPRs (a SIR-4000 with a 1.5 GHz antenna and a 2.6 GHz-Structurescan from GSSI manufacturer), and a wideband 3D GPR (from 3D-radar manufacturer). Radargrams are processed with refined signal analysis to detect constructive interference between overlapping echoes. It was performed from timely data by a supervised machine learning method, namely support vector machines (SVM) [56], and the result is compared to the conventional reference method and the Amplitude Ratio Test (ART). In this latter, debonding detection requires computing the conventional ART as the ratio between the reflected wave (RW) and the direct wave

(DW), namely, ART = RW/DW for each A-scan [56], [57]. Data processing automatically picks the maximum (or minimum) amplitude of the two latter echoes with some existing commercial radar processing software. In terms of pavement monitoring related to any debonding provides additional echoes which mostly interact constructively with each other. Consequently, the amplitude of the GPR signal of the reflected signal (RW) compared to one of the healthy zones [57].

Based on the GPR signal, a novel methodology was developed to detect the delamination of thin air-gap caused by delamination, which usually is less than 2 cm thick [27]. A vehicle-mounted GPR system, consisting of two air-coupled antennas of 1 GHz and 2 GHz, respectively, and four 300 MHz ground-coupled antennas were used in this work. Obtained results have a good agreement with the core samples extracted from the same location. GPR can also be combined with other NDT methods for delamination detection on concrete bridges [59]. Other delamination detection studies using NDT, including GPR, are illustrated in the work of [7].

3.3 Subsidence and sinkholes detection

Subsidence seriously affects the structural stability and safety of pavements. Many causes can generate this type of problem, such as poor soil compaction, non-homogeneous consolidation and weak load-bearing capacity of soils, which seriously affect the conditions and mechanical behaviours of the foundation soils. When subsidence occurs, cracks, fractures, and potholes can appear on the pavement surface. Most seriously, in heavily loaded pavements, there is a risk of pavement sinking that can lead to collapse.

The solution to maintain both the integrity and stability of the pavement and foundation soils is the early detection of subsidence so that preventive actions can be carried out. In this context, the GPR provides an ideal solution to map sinkholes and settlements due to its high-resolution imaging without altering the soil structure while covering a vast area in a relatively short time with a reduced effort. One of the most followed guidelines, such as the ASTM-D6429 standard guideline [60], has also mentioned and included three primary geophysical methods for the investigation of sinkholes and voids: GPR, Frequency Domain Electromagnetic and Gravity.

[61] showed several GPR case studies on subsidence and sinkholes detection in urban areas affected by karstic processes. The GPR surveys were conducted using 500 MHz, 250 MHz, and 100 MHz shielded antennas. The GPR data produced allowed the identification of zones with subsidence processes and collapse geometry affecting different anthropic levels that were progressively accommodated (revealing continuous aggradation). One of the cases studies were carried out in a motorway with a shallow water table. In this case, anomalous asphalt thickness

was identified and considered as subsidence. [62] performed a GPR study with a 250 MHz shielded antenna to locate depressions and sinkholes in an area of old mine workings. From the GPR data produced, it was found that a sinkhole (which appeared at the surface a few months after measurements) was most certainly caused by the existence of an underground water channel and subsequently weakened strata. [63] showed a 400 MHz GPR survey used for air-void detection under a road. A subsurface void approximately 4 m long and 1.5 m deep was detected and confirmed by drilling boreholes. [64] presented a GPR study to characterise the ground conditions in an urban area, where subsidence occurred and was repaired. A shielded antenna with a frequency of 400 MHz was used for data acquisition, and the GPR data produced allowed to differentiate between loose and dense layers successfully. [65] used GPR shielded antennas with frequencies of 800 MHz and 500 MHz to map loose filling and subsidence in a port area consisting of stone paving blocks and "all-one" filling. 3D methodologies were used to provide reliable information about the actual extent of the anomalies. [66] presented a 3D GPR study using a 200 MHz shielded antenna focusing on detecting sinkholes in a collapsed urban area. It was possible to identify loose soil and cavities along a stretch of the road that could be affected by leakage and the water pouring into the layers. [67] included a 3D GPR study to detect sinkholes in a parking area where a sinkhole formation has collapsed in the past. For the survey, a 100 MHz shielded antenna was used, and the results revealed a large subsurface cavity that collapsed several months after measurements. [68] presented two different GPR case studies using a 400 MHz shielded antenna, (i) to investigate the area outside a warehouse and (ii) to investigate an adjacent area to a bus garage, which aimed to evaluate the buildings foundations and possible causes of the decay of their structural elements. For the first case study, poorly-compacted or eroded zones were detected in the shallow layers of the soil that suggests a settlement phenomenon at the shallow foundations; whereas for the second case study, it was possible to identify a soil area with greater water content; hence, this irregular distribution of water, and the absence of drainage systems, could be the cause of the settlement observed in the adjacent building. [69] carried out a GPR study to monitor an active sinkhole in an urban area. The survey was performed with both 100 MHz and 200 MHz shielded antennas. The results produced have revealed the internal structures of the sinkhole and approximate extent, while identifying boundaries of subsidence areas and deformation structures (collapse faults, fissures, etc.).

Figure 8 presents an example of subsidence detection with 500 MHz ground-coupled antennas. The GPR profile line was conducted along an area supporting trucks circulation and maneuvering. This area consists of a 20 cm reinforced concrete slab, followed just underneath by an anthropic filling. From the interpretation of the GPR data, it was possible to identify reinforcement

settlement (highlighted in dotted red lines), as well as a large subsidence in the middle of the B-scan (highlighted in the red ellipse) that compromises the stability of the soil system and, more importantly, could lead to collapse under heavy load conditions.

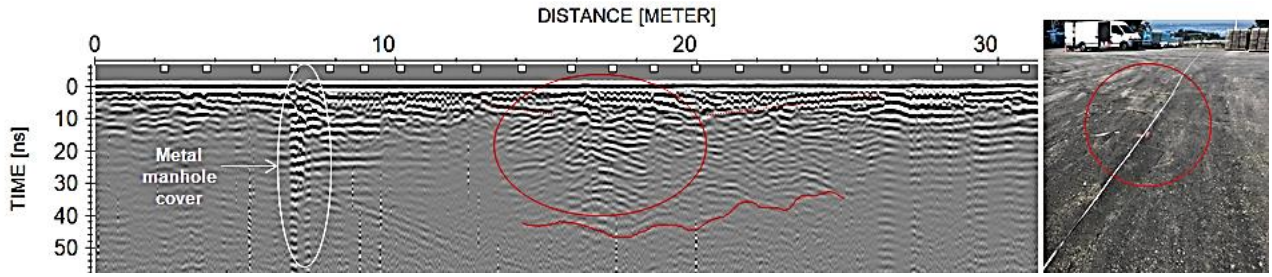

Figure 8. 500 MHz GPR data showing reinforcement settlement and filling subsidence (highlighted in red ellipse).

3.4 Moisture of granular and subgrade layers

One of the main causes of damage in pavements is the humidity in the asphalt and subgrade layers. The subgrade is the deepest layer of the pavement and supports the base and the asphalt layers. The water content in the subgrade may come from surface filtration through the cracks in the upper layers, from the subsoil water, or due to filtrations from the road's gutters. In all cases, incorrect drainage could damage the pavement because the subgrade reduces the bearing capacity when water accumulation saturates the soil.

The study of the subgrade layer is crucial to assure the proper conditions for the service life of the infrastructures. The analysis in railways to detect moisture in the subgrade demonstrates the technique's feasibility [70] . This work obtained the wave velocity in the subgrade from common mid-point data acquisition, determining the velocity curves and gradients. The humidity is estimated from those velocities using the Topp relationship [71] . The dielectric permittivity from aggregate sub-bases was also determined by comparing amplitudes of the reflected waves [72] . The gravimetric water content was estimated from a relation between the moisture content, densities and dielectric permittivity of aggregates and base materials [73]. In other cases, the identification of reflections allowed to determine the wave velocity used to analyse the water content comparing the two-way travel time in radargrams to the layers observed in cores. The accuracy of this method is higher as more samples are obtained [31] . However, due to the noise, humidity in the pavement layers is difficult to determine only using GPR, and complementary methodologies are recommended [74], being GPR mainly used to determine the water content in the soil under the pavement. In general, GPR is recommended to determine the water content and soil substructure under roads because the permittivity estimated with GPR is sensitive enough to detect differences in soil materials, moisture content, and the presence of frost in soils used to construct roads [75]. The surveys with high-frequency antennas (higher than 2 GHz) allows a more

accurate analysis of the pavement layers, being in some cases possible to develop algorithms for rapid pattern recognition, detecting automatically damaged zones [76].

Changes in the frequency of the reflected signals can also highlight the existence of moisture in the base of pavements [42] because an increase in the gravimetric water content produces a displacement of the maximum amplitude peaks of the spectrum to lower frequencies. Figure compares the spectrum from a dry sector with the spectrum obtained in a road with significant damage due to water content in the subbase and a reference spectrum. The study was performed with an 800 MHz centre frequency antenna, analysing the granular subbase of the pavement.

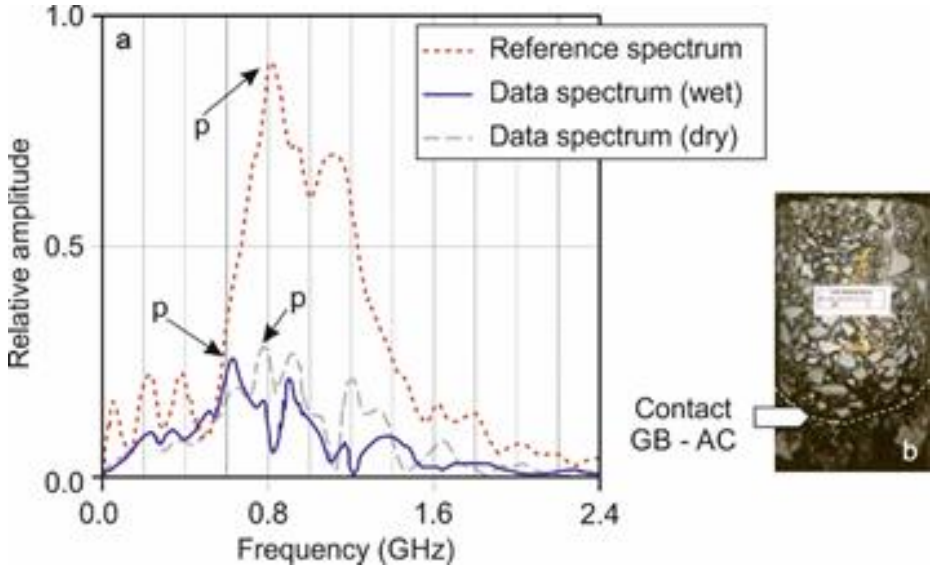

Figure 9. Spectrum of dry and wet pavement base. a) Reference spectrum compared to the spectra from data obtained in dry and wet sections. b) Sample showing the contact between the asphalt concrete (AC) and the granular subbase (GB) (modified from[42])

The peak corresponding to the maximum amplitude in the reference spectrum is placed around 800 MHz. In the dry granular subbase, the peak is slightly moved to a lower frequency but the peak has a significant move to the lower frequency for wet granular subbase.

Based on frequency analysis and dielectric permittivity estimation, the development of automatic detection of humidity is a challenge. [77] carried out deep learning approaches with promising results.

3.5 Underground utilities assessment

Critical infrastructures such as transportation networks, water, electricity, among others, are essential systems for the development of cities. The proper operation of these critical infrastructures depends not only on the components of the system itself but also on the adequate functioning of the components of their interconnected systems. For example, failures of pipes in either water collection systems or water distribution networks can lead to prolonged disruptions

(or also collapse) in parts of the city for the services in both the water and road infrastructure [78], [79]. Thus, in road pavement inspection and given its close relationship with buried assets of buried infrastructures i.e., drinking water pipes, drainage pipes/water collection (e.g., rainwater and sewage pipes), gas pipelines [80], among others., the development of reliable assessment/monitoring mechanisms for the health of buried assets (i.e. in particular for utility pipes) is gaining a main interest in cities. This development prevents/mitigates failures that can lead to potential economic, social, and environmental impacts in transportation and utility systems [81] . One of the most common methods used for health assessment and characterisation of buried pipes is the GPR [80], [82]. In this sense, this section explores the use of GPR in buried pipes for both characterisation and health assessment, focusing on drainage pipes in the context of urban roads.

In general, GPR applications for pipes (some examples of these applications are presented in Figure .10):

- the utility mapping (e.g. detection of pipe layouts, pipe size, pipe depth);
- pipe wall thickness estimation;
- identification of the state condition of the pipe by detecting each anomaly/defect within pipe wall (e.g. pipe wall fractures, corrosion in case of metallics pipes, pipe-bursting) [83];
- identification of water leakage and mapping cavities in surrounding pipe areas [80].

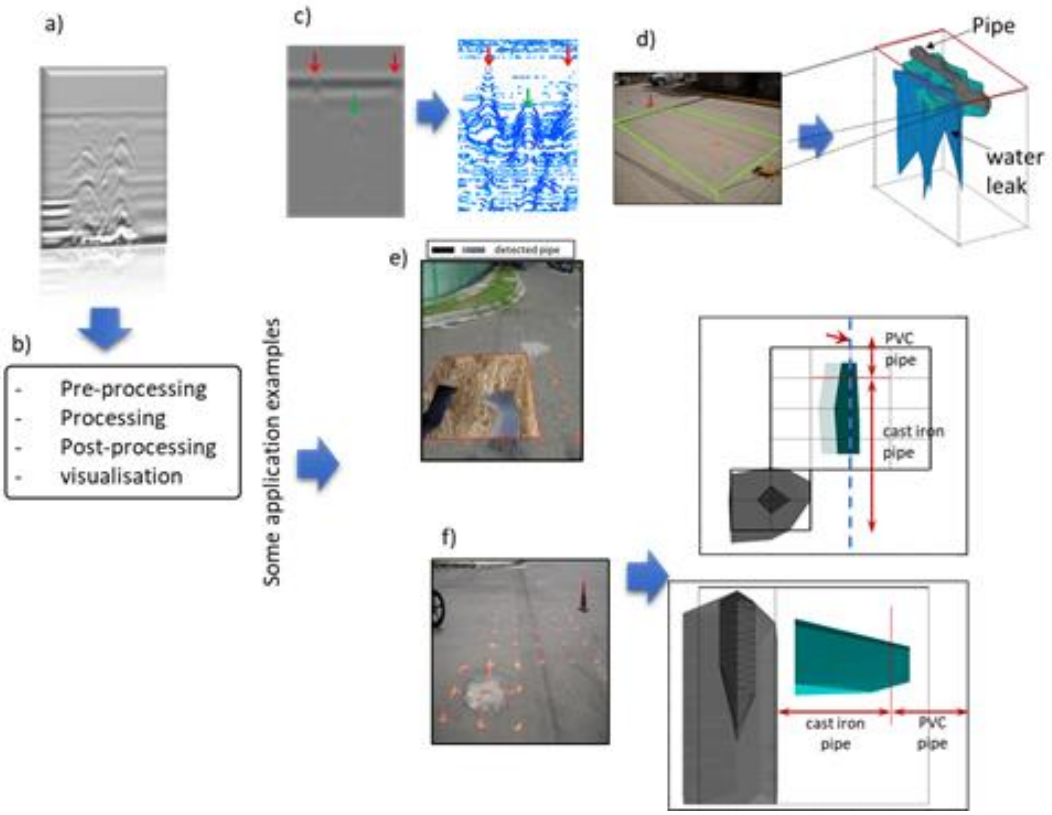

Figure10 A few GPR application examples for pipes assessment. a) Raw GPR images, b) treatment and interpretation, and c-f) applications. c) Characterisation of plastic pipes, d) water leakage detection and characterisation of the leak phenomena, e) visualisation - augmented reality, and f) 3D retrieval. (Adapted from [[84]–[87])..

Due to the dielectric differences between the material and the areas surrounding it, a contrast is generated, mainly in the relative dielectric permittivity, facilitating the pipes' identification (detection) in images captured using GPR [88]. Numerous authors take advantage of this principle in order to map the water-related pipes. Thus, [89] reported some GPR studies to detect buried utilities, among which stands out the use of a frequency antenna ranging from 100MHz to 1500MHz (in particular 100, 200, 250, 270, 300, 400, 500, 700, 800, 900, and 1500 MHz) for asset depths between 8cm-163cm in real urban environments. [89] uses a kinematic GPR (with central frequency of the antenna of 400MHz) and self-tracking (robotic terrestrial positioning systems - TPS) for identifying the layouts and also the characteristics (material, diameter, depth, position) in urban environments. Evaluated assets include pipelines (drinking water, plumbing water, industrial water, sewage, heating - culvert), gas, electrical and signal cables, with different pipe materials (polyethene, concrete, ductile iron, ductile cast iron, glass reinforced polyester), for diameter of 31mm-400mm and depth ranges of 80cm-350cm. The layers of the real urban sites include materials such as asphalt concrete and granular base.

Similarly, [90] used a multi-channel GPR unit (34 transmitter-receiver with a frequency of 600MHz), combined with a Global Navigation Satellite System (GNSS) with the support of pulse per second (PPS) and total station to identify the location of the utilities in urban settings. Pre-location of pipe layout for the sewage system was conducted by identifying visible components (e.g., drainage grille, metal tape) and then GPR confirmation was performed. Although the authors highlight the uses of GPR in layout detection for sewage pipes, they also noted the reduction in detection efficiency for pipes with large diameters located at depths for the frequency of the antennas used.

In order to characterise pipes (i.e., estimation of depth, diameter, content and eventually the pipe layout) for drainage systems embedded in concrete pavement, [82] coupled simulated GPR images (i.e., using the finite-difference time-domain (FDTD) method) and migration reconstruction method. Internal pipe condition is another topic of particular interest in water-related pipes. Thus, there are some studies based on amplitude analysis, as in [91] developed in water sewage systems with GPR (with a central frequency of the antenna of 2.6 GHz) in asbestos cement pipes (out of service pipes) of different ages, diameters (from 300mm to 525mm) and thicknesses (from 24.1mm to 40.6mm) for pipe health assessment (estimation of wall thickness and pipe state). [92] estimated the corrosion rates in cast iron pipes using GPR through numerical simulations and based on hyperbolic reflection analysis. The formation of underground voids in surrounding pipe areas was studied in[93] and [94] to preserve the structural integrity of sewerage pipes. The first uses FDTD in its studies, while the second performs a cavity mapping using a 400MHz in a real urban

environment. To evaluate pipes within themselves, [95] coupled a GPR (antenna frequency used: unknown) with the digital scanning and evaluation technology (DSET) to detect both geometric anomalies and property changes (potential pipe defects) for the assessment of underground sewage pipe condition. The GPR system in this case is used to facilitate the detection of anomalies that are difficult to appreciate by the human eye through the DSET system. Similarly, [83], [96] addressed the pipe assessment of voids within and outside, as well as the defect in pipes by using a GPR system (antennas with frequency of 1.6 GHz to 2.3 GHz were used) incorporated in a robot that performs the inspection inside the pipe. In addition, the detection of the deep underground small size pipe positions, and localise them is a challenge task in the assessment of critical infrastructures. The detection of such pipes depends on the GPR antenna freauency, and subsurface conditions, mainly wet, dry, contaminated. Use of intelligent data analysis, such as machine learning or deep learning could be efficient in order to increase the accuracy of the radar images [97], or combination of GPR with other possible non-destructive evalautions (NDE) [98].

4. Incorporation of GPR with other methods for pavement assessment

As addressed in the previous sections, the GPR method represents an essential non-destructive pavement structural assessment tool. It allows for the continuous detection of layer thicknesses and locating defects and inner damages such as cracking, delamination or subsidence. In addition to the GPR for providing layer thickness information, other complementary devices such as accelerometers and laser scanning profilometers are generally used to measure the road texture and roughness for quality control and quality assurance [99]. GPR was combined with infrared thermography to detect cracking and shallower delamination in asphalt pavements [50] and inner defects (lack of filling and subsidence) in paving blocks roads [65].

Another NDT technique commonly used together with the GPR for the structural evaluation of pavements is the FWD, which allows evaluating the bearing capacity of pavements based on loading tests. The FWD simulates the pavement responses under traffic loading by applying an impulse load and then measuring the pavement deflection bowl. The standard procedure is to measure the deflections in a considerable number of points located along several lines parallel to the pavement axis (the same test lines as the GPR) and spaced in 50 to 200 m [54]. Thus, layer modulus (strength of each layer) can be estimated throughout back-calculation using the deflection values measured by FWD and the layer thickness obtained from GPR. Examples of published articles combining GPR with FWD are [11], [100]–[102]. New loading tests devices were developed for monitoring at high traffic speed, such as Traffic Speed Deflectometer (TSD) [103], [104].

Figure 11 shows three examples on the combination of different NDT data for pavement assessment. First, **Erreur ! Source du renvoi introuvable.**11-a) presents two graphics showing both the International Roughness Index (IRI) profile and the GPR layer thicknesses profile produced for the same profile line. Next, **Erreur ! Source du renvoi introuvable.**11b) displays the orthothermogram produced in the shallower subsurface (2-5 cm depth) of a paving blocks road and the 3D GPR time-slice obtained at 2 m depth in the grid. The IRT image shows the interpretation of some areas having higher temperature (highlighted into red boxes) At the same time, the GPR data allows to detect an inner subsidence (lack of filling or cavity) that extends from 0.5 to 2.0 m depth, coinciding with one of the anomalies interpreted by the Infrared Thermography (IRT) method (box n. 6). Finally, **Erreur ! Source du renvoi introuvable.** 11-c) illustrates a comparison and integration of both FWD deflections (D0 to D3) and GPR B-scan (2.3 GHz ground-coupled antenna) for the same profile line (the yellow ellipses indicate anomalies in the GPR data). The discontinuity observed between deflections D2 and D3 at 7.5 m (C1) was interpreted as cracking or debonding of the subgrade layers. In comparison the higher difference between deflections D0 and D1 at 9.0 m (C2) was associated with cracking on the top layer.

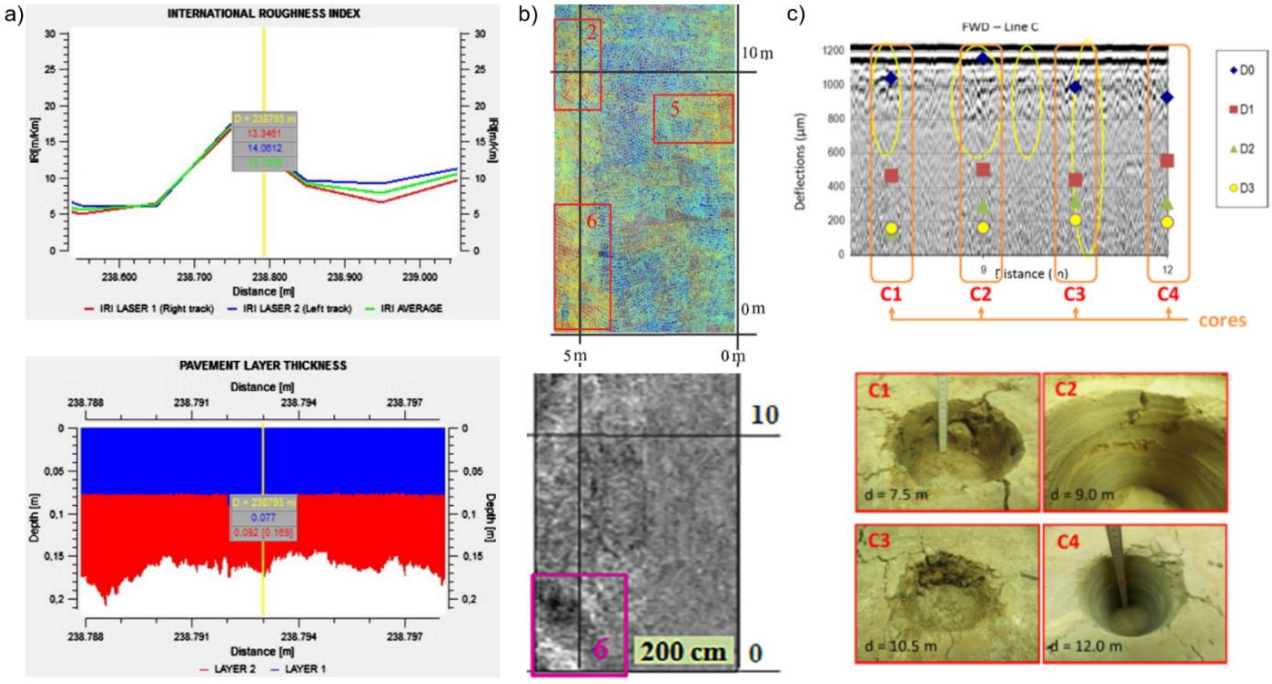

Figure 11 Examples of the combination of different NDT techniques for pavement evaluation: a) IRI- roughness profile and layer thicknesses profile obtained by GPR; b) IRT and 500 MHz GPR data (time-slice at 2 m depth) highlighting a subsidence (box n. 6); and c) FWD and 2.3 GHz GPR data to detect cracking and debonding. Adapted from [11], [65], [105].

Concerning the stability of the pavement structure, the Electrical Resistivity Tomography (ERT) is combined with GPR aiming to assess the soil compaction, cavities and the depth and condition of the bedrock [106], [107]. Another geophysical technique widely used together with GPR in pavement assessment and geotechnical road stability is the Seismic Refraction Tomography (SRT)

[108], [109]. The seismic method allows for deeper investigations than GPR to assess geological hazards (subsidence phenomena, cavities, fractures in rocks, etc.).

The use of a multi-temporal Interferometric Synthetic Aperture Radar (InSAR) for pavement assessment has also been significantly increased during the last few years [110]. In this regard, some works in the literature [111], [112] show the potential of the applicability of the InSAR technique to monitor differential settlements as well as, together with GPR, to outline subsidence areas.

Regarding concrete pavements, especially in bridge decks, most of the published literature focuses on delamination. Thus, it was possible to find some articles dealing with the combination of GPR with acoustic surveys. [113] revealed that the acoustic method detects near-surface delamination, while GPR can penetrate concrete thus proving deterioration in depth. Another NDT technique used in conjunction with GPR on delamination assessment is the IRT method. Once again, the orthothermograms detect near-surface delamination under convenient weather conditions, while GPR allows for deeper investigation [114] Both impact-echo and pulse-echo techniques are widely used to detect delamination and other defects such as voids and cracks [115], [116]. Other methods such as half-cell potential (HCP), electrical resistivity (ER) and hammer sounding resistivity, are used in combination with GPR and/or ultrasonic surveys to analyze corrosion and its spatial distribution in areas affected by delamination [117], [118].

5. GPR-based Machine Learning and Intelligent Data Analysis approaches

Numerous efforts have been made to increase the interpretability of GPR data to make this information more accessible, less dependent on interpretation skills for the persons responsible to conduct assessment on transport systems, and ultimately to facilitate the decision-making process. GPR appears to be an efficient method capable of providing road transportation systems with reliable information on the infrastructures' health and surroundings using non-destructive equipment. GPR data analysis requires expert experience in the treatment of this type of data. This treatment requires methods that automate the interpretation process, making it feasible and applicable to large-scale systems [119]. Therefore, advances in data analysis reduce analysis times and minimise the human errors involved in this process [120]. This section explores machine learning (ML), deep learning (DL) and the intelligent data analysis (IDA) methods applied to GPR data for road transport infrastructure inspection.

The main objective of the use of ML apparoaches is an alternative approach to more traditional, but computationally more expensive, algorithms, trained models which can usually be applied only to a post-processing radar data. Certainly, in literature ML has already been proved as an effective

approach to GPR various civil engineering applications in both aspects; detection and classificationof the buried objetcs [121], [122]. The main approaches were used from different researcher (i.e., pre-processing, segmentation approaches, and feature extraction). In this paper mainly, modern deep learnig approaches are considered and indicated based on litreture. On the other hand, dealing with GPR images is a challenged task, and using various approaches beside deep learning is crucial to increase the interporbility of the radar images, and increase the probability detection of the embeded target considering reliability of the data-driven from the field, controlled laboratory or numerical models. Table 3 shows some examples of the efforts conducted to incorporate IDA methods to increase the interpretability of the GPR data and transform this data into valuable information [123]. Aspects addressed through IDA approaches related to road inspection include object detection, cavity detection, pavement distress detection, grade classification of loose damage, pavement cracks, moisture damages, and thickness estimation. In addition, other relevant aspects should be considered in the GPR data analysis, such as data acquisition/generation, clutter removal reduction [37], [124] and reduction of medium inhomogeneity [125] that have been addressed in IDA methods.

The interpretation of GPR images typically comprises the development/adaptation of ad-hoc filters that get understandable the information collected. In this sense, the application of deep-learning methods, particularly convolutional neural networks (CNN), stands out. In these systems, data is synthesized through several filters (kernels) within different layers in a feature map that condense the relevant information gathered from the initial inputs. The feature maps obtained are the basis for other processes such as classification, detection and prediction. Pre-trained network architectures such as AlextNet is considered in order to facilitate the CNN training process [37], [125]–[127], Darknet53 [120], Cifar-10 (on grayscale) [128] and ResNet50 [129], which have been adapted by using transfer learning methods for the feature extraction of GPR images. A part or entire pre-trained network's architecture (including the weights) is adapted either for automatic characterisation or target detection. For example, [123] a coupled CNN with Long Short-Term Memory (LSTM) is used, which is a model of Recurrent Neural network (RNN) for the automatic identification of the diameter of buried cylindrical object. An equivalent method to the CNN which is based on wavelet transformation with the rotation and translation of invariant operators, called wavelet scattering network, is also used to extract GPR images [130] .

Following the feature extraction methods, there is the detection/classification process. Detection algorithms such as Soft-max in[120], [127] and You Only Look Once (YOLO) in [119], [129], [131], where a multi-label classification is used for GPR imagery purposes. Furthermore, Faster-region convolutional neural network (Faster-RCNN) for buried objects detection with a few

training samples is proposed [128] and for pavement distress detection in [132]. Inspired in YOLO algorithm in [18] which is proposed as a single-stage object detector. A Support Vector Machine (SVM) with the uses of radial basis function is used for classification in [130] and [133]. Alternative method using the traditional three-point circle method (denoted as "three-point rounding") for automatic identification of buried pipes (e.g., diameter and position) is proposed in [134]. A procedure to increase the cavity detectability on roads that includes the CNN, super-resolution (SR) generation and automated classification phase is also proposed in [126] and [135], [136] used back-propagation (BP) neural network for the automatic classification and recognition of looseness in base.

The process of gathering adequate data sets that enable the training, fine-tuned, and validation of the above-mentioned intelligent system is a challenge task. In this sense, the most common strategies involve the field surveys, experimental samples, and artificial generation of GPR data based on simulation or combination of various data sets. Field data collection of GPR images (e.g., see [77], [128], [136]), in some cases, data acquired by a vehicle-mounted GPR system (e.g., [119], [120], [126], [127], [131], [137]) which has been used as a strategy for GPR dataset preparation for inspection of roads in urban environment. Similarly, the use of experimental samples to collect the GPR images is highlighted (e.g., tank configuration [123], [136]). laboratory experiments of GPR dataset are conducted in order to maintenance or re-install buried objects in urban areas. For instance, the GPR information is used for the detection algorithms (e.g., see open database of radargrams in [138] as used in [130] , or in [139] as used in [136]). The use of FDTD method is a complementary approach to validate GPR dataset driven from field or/and laboratory in a simulated form. This can also feed the pattern extraction systems; e.g., in [136] a FDTD code is usually generated in MATLAB to obtain simulated GPR images of embedded features in pavements. Several research studies have been investigated on the similar topics such as [53], [76], [123], [128], [130], [134] , use the gprMax software [140], [141] which is based on FDTD to solve maxwell's equations in order to obtain simulated GPR images of buried objects e.g., pipes, rebars, and complement/develop their datasets.

Several researches support their own IDA process in a pre-treatment of the information to facilitate the feature extraction process. Among this, a technique of the signal amplitude thresholding (determination of upper and lower signal to separate targets from the background) is investigated [120]. Similarly, in order to delimit the regions of the GPR image where the target object is embedded in [123], the use of an adaptive target region detection (ATRD) algorithm is proposed. By removing the linear features from GPR images, i.e., consequently increasing the visibility of buried objects in them, in [127] an algorithm denoted by the authors as "basis pursuit-based

background filtering" was developed. In [130], two pre-processing methodologies "dewow" and "amplitude gain" are used. The first "dewow" is applied to remove the effects of the occurrence of low-frequency noise components within each GPR image. The second filter (amplitude gain) is to improve the signal for the attenuation in particular for the latter arrived signals. To extract the signal attributes from GPR images which have a correlation with the loose damage, in [136] a signal eigenvalue extraction method is used. A series of pre-processing treatments is included among others, inverse Discrete Fourier Transform, and background removal are applied in [77], [131].

Also multi-agent systems supported by game theory have been proposed in [142] with the so-called "race agent" algorithm. This algorithm has the premise of seeking data reduction, while preserving the characteristics of the elements embedded into the GPR images. With the use of this pre-processing method both classification and visualisation processes are facilitated. Figure 12 presents an example for the extraction of water leakage patterns by the uses of both the "race-agent" algorithm and classification by means of perceptron neural network. Some examples of the uses of this algorithm are, for example, the automatic detection of plastic pipes [143], the characterization of water leaks [84], and the extraction of patterns that allow understanding and anticipating the water leak phenomenon in urban water infrastructures [97].

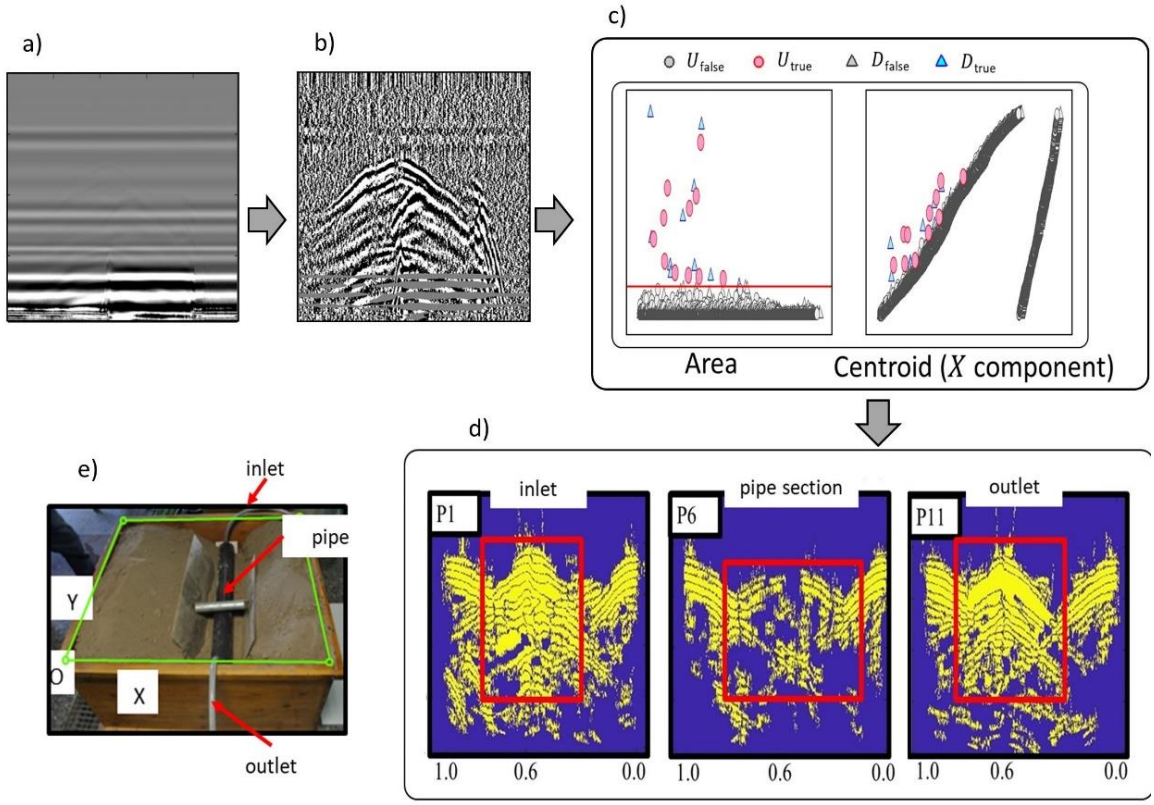

Figure 12 An example of pre-processing and extracting water leak patterns from GPR images. a) Raw GPR image, b) pre-processed matrix using agent-race algorithm, c) data families and data labelling, d) families classified by perceptron neural network, and e) setup for water leak capture. (Adapted from [97]).

Data augmentation is proposed in order to increase the quality, diversity and size of the GPR datasets[119]; This technique preserve the input target labels considering the input transformation. Shifting an original GPR image has been used in [125], [127] in order to augmented the dataset. More robust methods are investigated to augment the data and increase the quality of this data includes the Generative Adversarial Networks (GANs) [136], [144] or incremental random sampling (IRS) [77]. Although many efforts have been made with the aim of automating the tasks of inspection and monitoring of the roads. The reliable autonomous interpretation of the GPR records remains a paramount in the nowadays research projects. In addition, IDA approaches have been proven to be an efficient tool that can facilitate this process in its different stages (Table 3).

Table 3. An overview of road inspection methods that use GPR and incorporate intelligent data analysis

Inspection task	References	Data set preparation	Pre-processing	Feature extraction	classification/ detection	Target
Object detection - characterisation of objects embedded in transport infrastructures	[120]	Field data collection	Thresholding of signal amplitude. Manual labelling of data library	CNN		Automatic classification of the hyperbola, manhole cover, layer interface and subsoil background.
	[119]	Field data collection	Data Augmentation. Manual labelling of data library	CNN	YOLO model	Automatic classification of rainwater wells, cables, non-metallic and metallic pipes, steel reinforcement.
	[123]	Numerical simulations and field data collection	ATRD	Ensemble of CNN and LSTM		Automatic diameter identification of the cylindrical buried objects
	[130]	Numerical simulations and experimental open GPR datasets	de-"wow" and amplitude gain	Wavelet scattering network	SVM	Automatic pipe location and diameters for non-intensive data sets
	[128]	Numerical simulations and field data collection	-	CNN	Faster-RCNN algorithm	Automatic detection of buried objects with few training samples
	[136]	Numerical simulations, field data collection and open GPR datasets.	GANs	Single-stage object-detector		Automatic buried objects detection via hyperbola detection, attempts to address the scarcity of GPR data.
	[134]	Numerical simulations	-	-	"Three-point	Automatic identification of buried pipes (e.g.,

					rounding" method	diameter, and position)
Damage detection on transport infrastructure	[127]	Field data collection	Shifting and "basis pursuit-based background filtering" algorithm	CNN		Automatic underground cavity identification in roads
	[126]	Field data collection	-	CNN, Super resolution image generation, and automated classification phase		
	[132]	Field data collection	-	Faster-RCNN algorithm		Automatic pavement distress detection
	[144]	Numerical simulations	Signal eigenvalue extraction	BP neural network		Automatic classification of loose damage
	[131]	Field data collection	Filtering	YOLO model		Automatic recognition and location of concealed cracks in pavements
	[77]	Field data collection	Filtering and IRS	CNN	YOLO model	Automatic moisture detection and location
	[133]	Numerical simulations	-	SVM		Layer thicknesses estimation

The limitation of IDA methods depends on the reliability of the GPR data set, and amount of the data which can be trained and tested, and based on these, the validation and the accuracy of the trained model is essential in order to provide an effective tool. Therfore, the interporbiolity of the ML results to a decision maing model which can be used from owners/opertaors of the road transport infrastructures in an easy predictive model, which require some IDA expertise.

6. Remarks and Further trends

GPR is nowadays a consensual tool for continuous layer thickness assessment at traffic speed. Moreover, several other essential pavement characteristics for structural monitoring can be observed, such as settlements, layers debonding and water presence.

The main challenge for continuous structural monitoring is the data processing interpretation and integration due to the significant volume of information gathered during GPR data acquisition.

Building Information Modelling (BIM) developments as a tool that can integrate the evaluation results in an updated pavement model are also addressed. The BIM model automatically integrates the B-scan results that can reflect the evolution of pavement condition along the life cycle and

represent a base for performance indexes development and validation [145]–[147]. Automated and new technologies such as machine learning, digital twins, and robotic platforms are widely conducted. Lately, there have been many innovative research projects funded by various institutions in Europe and globally. They provide better road transport infrastructures, mostly thus are robotic inspection and real-time monitoring approaches of various research gaps in the field of road pavements. Some of the above-mentioned projects are illustrated in Table 4.

Table 4. On-going innovative research projects in the assessment of the road transport infrastructures.

No.	Project Acronym	Title	Description	Funded by
1	CoDEC	Connected Data for Effective Collaboration	To study the key means for successful implementation of Building Information Modelling (BIM) principles within the European highways industry, in particular with regards to freeing and enriching data flow to and from Asset Management Systems (AMS)	CEDR (Conference of European Directors of Roads) under grant agreement no 859887 (https://www.codec-project.eu/)
2	PANOPTIS	Development of a Decision Support System for increasing the Resilience of Transportation Infrastructure	To improve the resiliency (ability to adapt) of the road infrastructures and ensuring reliable network availability under unfavourable conditions, such as extreme weather, landslides, and earthquakes.	Horizon 2020 research and innovation programme under grant agreement no 769129 (http://www.panoptis.eu/)
3	HERON	Improved Robotic Platform to perform Maintenance and Upgrading Roadworks	To develop an integrated automated system to perform maintenance and upgrading roadworks, such as sealing cracks, patching potholes, asphalt rejuvenation, autonomous replacement of CUD elements and painting markings, but also supporting the pre/post-intervention phase including visual inspections and dispensing and removing traffic cones in an automated and controlled manner.	Horizon 2020 research and innovation programme under grant agreement no 955356 (http://www.heron-h2020.eu/)

One another significant future trend is the use of remote sensing to monitor settlements of pavements. It is helpful as it is available free of costs by European satellites (Copernicus European Program). The combination of satellite data with radar images is crucial to interpret the service state of pavements better. Several studies performed on pavement evaluation have proven this approach's efficiency, mainly on subsidence and road profile [110], [148], [149].

The importance of advanced monitoring technology that integrates interpretation and modelling are highlighted as tools for pavement management systems. It provides a confident diagnosis of the structural condition of existing pavements and enables economically efficient maintenance that guarantees the pavement's proper behaviour and an extended life cycle. Following the previous sections, GPR is an NDT method that makes it possible to assess the pavement's structural health

and service state, and therefore to make rational decisions in terms of management, maintenance, repair actions, and cost analysis to the road pavement. As for other NDT, the objective is to optimize the decisions, which means making the most possible best decision at the best time to maximize its impact while minimizing the cost of repair and maintenance. Several cases of GPR use for decision-making purposes already exist in the literature. Table 5 presents two cases studies related to the use of decision-making approaches based on GPR data. These cases are linked to the road pavement itself (repair actions for cracks, treatment of water in the pavement, cleaning and routine maintenance actions, etc.) and to networks embedded in the pavement (water works, electricity or gas supply, etc.). Using various and suitable types of data analysis could be a key support to provide valuable structural health knowledge on pavements, leading to an optimised approach for repairs and maintenance. The use of GPR is still localized, both in time and in space and can be a useful support for decision-making owners/operators. The future of the use of GPR might be the routine and scheduled use of GPR, combined with other sensors and installed on automated vehicles, for continuous and real-time assessment of the road infrastructure and application of response actions.

Table 5. Summary of previous studies related to decision-making methodologies based on GPR data for road pavements

No.	Problematic (Hypothesis)	Approach	Use of GPR technology	Remarks	Reference
1	Use of GPR technology to provide quantitative information for improved decision making and reduced operating costs.	Multi-scale pavement GPR data Analysis (MPGA)	Yes	The testing and demonstration showed significant potential for quality control using GPR.	[150]
2	A real case study, focusing on a set of GPR images for optimizing maintenance management of Water Supply Systems	Multi-criteria decision making (MCDM)	Yes	Significant results are shown on the decision-making approach based on GPR data	[151]

CRediT authorship contribution statement

Coordination of the project: Mezgeen Rasol, **Conception:** Mezgeen Rasol, Jorge Pais and Merceds Solla. **Writing, Reviewing, Materials, and Revision process:** Corresponding authors, and all co-authors has been equally participated in developing, writing, revising and reviewing this review paper.

Acknowledgement

This project has received funding from the European Union's Horizon 2020 research and innovation program under grant agreements No. 769129 (PANOPTIS) and No. 955356 (HERON). The project has also partially supported by the GAIN, Xunta de Galicia, through the project ENDITí (Ref. ED431F 2021/08). Rasol M. acknowledges the financial support from Gustave Eiffel University, and Solla M. acknowledges the grant RYC2019–026604–I funded by MCIN/AEI/10.13039/501100011033 and by "ESF Investing in your future".

Conflicts of Interest

Authors declare there is no conflict of interest. The funders had no role in the design of the study; in the collection, analyses, or interpretation of data; in the writing of the manuscript, or in the decision to publish the results.

References

[1] P. Pereira and J. Pais, "Main flexible pavement and mix design methods in Europe and challenges for the development of an European method," *J. Traffic Transp. Eng. (English Ed.*, vol. 4, no. 4, pp. 316–346, Aug. 2017, doi: 10.1016/J.JTTE.2017.06.001.

[2] I. L. Al-Qadi and S. Lahouar, "Measuring layer thicknesses with GPR - Theory to practice," *Constr. Build. Mater.*, vol. 19, no. 10, pp. 763–772, 2005, doi: 10.1016/j.conbuildmat.2005.06.005.

[3] ASCE, "Standard Guidelines for the Collection and Depiction of Existing Subsurface Utility Data," Aug. 2021.

[4] R. L. Sterling *et al.*, "Encouraging Innovation in Locating and Characterizing Underground Utilities," Washingthon, DC, 2009. doi: https://doi.org/10.17226/22994.

[5] F. M. Fernandes, A. Fernandes, and J. Pais, "Assessment of the density and moisture content of asphalt mixtures of road pavements," *Constr. Build. Mater.*, vol. 154, pp. 1216–1225, Nov. 2017, doi: 10.1016/J.CONBUILDMAT.2017.06.119.

[6] M. A. Rasol, V. Pérez-Gracia, M. Solla, J. C. Pais, F. M. Fernandes, and C. Santos, "An experimental and numerical approach to combine Ground Penetrating Radar and computational modeling for the identification of early cracking in cement concrete pavements," *NDT E Int.*, vol. 115, no. May, 2020, doi: 10.1016/j.ndteint.2020.102293.

[7] M. Solla, V. Pérez-Gracia, and S. Fontul, "Review of GPR application on transport infrastructures: Troubleshooting and best practices," *Remote Sens.*, vol. 13, no. 4, pp. 1–5, 2021, doi: 10.3390/rs13040672.

[8] A. M. Alani, F. Tosti, L. B. Ciampoli, V. Gagliardi, and A. Benedetto, "An integrated investigative approach in health monitoring of masonry arch bridges using GPR and InSAR technologies," *NDT E Int.*, no. May, p. 102288, 2020, doi: 10.1016/j.ndteint.2020.102288.

[9] A. Benedetto and L. Pajewski, *Civil Engineering Applications of Ground Penetrating Radar*. 2015.

[10] V. Sossa, Vega Peréz-Gracia, R. Gonzalez-Drigo, and M. A. Rasol, "Lab Non Destructive Test to Analyze the Effect of Corrosion on Ground Penetrating Radar Scans," 2019.

[11] V. Marecos, M. Solla, S. Fontul, and V. Antunes, "Assessing the pavement subgrade by combining different non-destructive methods," *Constr. Build. Mater.*, vol. 135, pp. 76–85, 2017, doi: 10.1016/j.conbuildmat.2017.01.003.

[12] C. Plati, A. Loizos, and K. Gkyrtis, *Assessment of Modern Roadways Using Non-destructive Geophysical Surveying Techniques*, vol. 41, no. 3. Springer Netherlands, 2019.

[13] M. A. Rasol, V. Pérez-Gracia, F. M. Fernandes, J. C. Pais, M. Solla, and C. Santos, "NDT assessment of rigid pavement damages with ground penetrating radar: laboratory and field tests," *Int. J. Pavement Eng.*, vol. 0, no. 0, pp. 1–16, 2020, doi: 10.1080/10298436.2020.1778692.

[14] V. Salinas Naval, S. Santos-Assunçao, and V. Pérez-Gracia, "GPR Clutter Amplitude Processing to Detect Shallow Geological Targets," *Remote Sens.*, vol. 10, no. 1, p. 88, 2018, doi: 10.3390/rs10010088.

[15] M. Solla, H. Lorenzo, A. Novo, and J. C. Caamaño, "Structural analysis of the Roman Bibei bridge (Spain) based on GPR data and numerical modelling," *Autom. Constr.*, vol. 22, pp. 334–339, 2012, doi: 10.1016/j.autcon.2011.09.010.

[16] Rasol M,.Development of New GPR Methodologies for Soil and Cement Concrete Pavement Assessment, Mezgeen Rasol,PhD Thesis. Polytechnic University of Catalonia (UPC), 2021.

[17] B. Riveiro and M. Solla, *Non-Destructive Techniques for the Evaluation of Structures and Infrastructure*. 2016.
[18] J. A. Huisman, S. S. Hubbard, J. D. Redman, and A. P. Annan, "Measuring Soil Water Content with Ground Penetrating Radar," *Vadose Zo. J.*, vol. 2, no. 4, p. 476, 2003, doi: 10.2136/vzj2003.4760.
[19] S. Satnley and scullion Thomas, "Development of ground-penetrating radar equipment for detecting pavement condition for preventive maintenance," *NDT E Int.*, vol. 28, no. 5, p. 311, 1995, doi: 10.1016/0963-8695(95)90104-3.
[20] D. G. Smith and H. M. Jol, "probable depths of penetration in Quaternary sediments," *J. Appl. Geophys.*, vol. 33, no. 1–3, pp. 93–100, 1995, doi: 1016/0926-9851.
[21] S. Al-Qadi, I. L., & Lahouar, "Use of GPR for thickness measurement and quality control of flexible pavements," *J. Assoc. Asph. Paving Technol.*, vol. 73, pp. 501–528, 2004, [Online]. Available: https://trid.trb.org/view/750001.
[22] S. Lahouar and I. L. Al-Qadi, "Automatic detection of multiple pavement layers from GPR data," *NDT E Int.*, vol. 41, no. 2, pp. 69–81, 2008, doi: 10.1016/j.ndteint.2007.09.001.
[23] ASTM D4748-10, "Standard Test Method for Determining the Thickness of Bound Pavement Layers Using Short-Pulse Radar, ASTM International," West Conshohocken, PA, 2020. doi: 10.1520/D4748-10R20.
[24] C. Gregoiree, A. Van der Wielen, C. Van Geem, and J.-P. Drevet, "ME91/16: Methodologies for the Use of Ground-Penetrating Radar in Pavement Condition Surveys," *Belgian Road Res. Cent.*, vol. ME 91/16, 2016.
[25] Highways England, Transport Scotland, Llywodraeth Cymru, and NI Department for Infrastructure, "GG 101 Introduction to the Design Manual for Roads and Bridges," *Des. Man. Roads Bridg.*, no. Revision 0, pp. 0–13, 2018, [Online]. Available: https://www.standardsforhighways.co.uk/prod/attachments/7b057727-55ee-48e5-98ff-bc3084ef807c?inline=true.
[26] T. Saarenketo, "Recommendations for guidelines for the use of GPR in asphalt air voids content measurement," 2012.
[27] Z. Dong *et al.*, "Rapid detection methods for asphalt pavement thicknesses and defects by a vehicle-mounted ground penetrating radar (GPR) system," *Sensors (Switzerland)*, vol. 16, no. 12, 2016, doi: 10.3390/s16122067.
[28] H. Liu and M. Sato, "in situ measurement of pavement thickness and dielectric permittivity by GPR using an antenna array," *NDT E Int.*, vol. 64, pp. 65–71, Jun. 2014, doi: 10.1016/J.NDTEINT.2014.03.001.
[29] A. K. Khamzin, A. V. Varnavina, E. V. Torgashov, N. L. Anderson, and L. H. Sneed, "Utilization of air-launched ground penetrating radar (GPR) for pavement condition assessment," *Constr. Build. Mater.*, vol. 141, pp. 130–139, 2017, doi: 10.1016/j.conbuildmat.2017.02.105.
[30] I. L. Al-Qadi, S. Lahouar, and A. Loulizi, "Ground-Penetrating Radar Calibration at the Virginia Smart Road and Signal Analysis to Improve Prediction of Flexible Pavement Layer Thicknesses," no. 3, 2005, [Online]. Available: http://hdl.handle.net/10919/46647.
[31] A. Loizos and C. Plati, "Accuracy of pavement thicknesses estimation using different ground penetrating radar analysis approaches," *NDT E Int.*, vol. 40, no. 2, pp. 147–157, 2007, doi: 10.1016/j.ndteint.2006.09.001.
[32] A. De Coster, A. Van der Wielen, C. Grégoire, and S. Lambot, "Evaluation of pavement layer thicknesses using GPR: A comparison between full-wave inversion and the straight-ray method," *Constr. Build. Mater.*, vol. 168, pp. 91–104, 2018, doi: 10.1016/j.conbuildmat.2018.02.100.
[33] V. Pérez-Gracia, D. Di Capua, R. González-Drigo, and L. Pujades, "Laboratory characterization of a GPR antenna for high-resolution testing: Radiation pattern and vertical resolution," *NDT E Int.*, vol. 42, no. 4, pp. 336–344, 2009, doi: 10.1016/j.ndteint.2008.12.007.
[34] M. B. Widess, "HOW THIN IS A THIN BED?," *GEOPHYSICS*, vol. 38, no. 6, pp. 1176–1180, 1973, doi: 10.1190/1.1440403.
[35] S. Zhao, P. Shangguan, and I. L. Al-Qadi, "Application of regularized deconvolution technique for predicting pavement thin layer thicknesses from ground penetrating radar data," *NDT E Int.*, vol. 73, no. March 2015, pp. 1–7, 2015, doi: 10.1016/j.ndteint.2015.03.001.
[36] S. Zhao, P. Shangguan, and I. L. Al-Qadi, "Application of regularized deconvolution technique for predicting pavement thin layer thicknesses from ground penetrating radar data," *NDT E Int.*, vol. 73, no. March 2015, pp. 1–7, 2015, doi: 10.1016/j.ndteint.2015.03.001.
[37] J. Wang *et al.*, "Deep Learning-Based Rebar Clutters Removal and Defect Echoes Enhancement in GPR Images," *IEEE Access*, vol. 9, pp. 87207–87218, 2021, doi: 10.1109/ACCESS.2021.3088630.
[38] J. Liu, J. Zhao, X. Yang, X. Qu, X. Wang, and J. Liu, "A tangential approximation algorithm for measured data reduction of blade section curves," *Meas. J. Int. Meas. Confed.*, vol. 128, no. April, pp. 504–515, 2018, doi: 10.1016/j.measurement.2018.05.085.
[39] C. Le Bastard, V. Baltazart, Y. Wang, and J. Saillard, "Thin-pavement thickness estimation using GPR with high-resolution and superresolution methods," *IEEE Trans. Geosci. Remote Sens.*, vol. 45, no. 8, pp. 2511–2519, 2007, doi: 10.1109/TGRS.2007.900982.
[40] S. Guha, S. Kruse, and P. Wang, "Joint time-frequency analysis of GPR data over layered sequences," *Lead. Edge*, vol. 27, no. 11, pp. 1454–1460, 2008, doi: 10.1190/1.3011017.
[41] J. P. Rodés, A. M. Reguero, and V. Pérez-Gracia, "GPR spectra for monitoring asphalt pavements," *Remote*

Sens., vol. 12, no. 11, 2020, doi: 10.3390/rs12111749.

[42] J. Pedret Rodés, V. Pérez-Gracia, and A. Martínez-Reguero, "Evaluation of the GPR frequency spectra in asphalt pavement assessment," *Constr. Build. Mater.*, vol. 96, pp. 181–188, 2015, doi: 10.1016/j.conbuildmat.2015.08.017.

[43] C. Fauchard, P. Côte, E. Le Brusq, E. Guillanton, J. Y. Dauvignac, and C. Pichot, "Step-frequency radar applied on thin road layers," *J. Appl. Geophys.*, vol. 47, no. 3–4, pp. 317–325, 2001, doi: 10.1016/S0926-9851(01)00075-1.

[44] I. L. Al-Qadi, Z. Leng, S. Lahouar, and J. Baek, "In-place hot-mix asphalt density estimation using ground-penetrating radar," *Transp. Res. Rec.*, no. 2152, pp. 19–27, 2010, doi: 10.3141/2152-03.

[45] Z. Leng, I. L. Al-Qadi, and S. Lahouar, "Development and validation for in situ asphalt mixture density prediction models," *NDT E Int.*, vol. 44, no. 4, pp. 369–375, 2011, doi: 10.1016/j.ndteint.2011.03.002.

[46] F. Soldovieri, G. Prisco, and R. Persico, "A strategy for the determination of the dielectric permittivity of a lossy soil exploiting GPR surface measurements and a cooperative target," *J. Appl. Geophys.*, vol. 67, no. 4, pp. 288–295, Apr. 2009, doi: 10.1016/J.JAPPGEO.2008.09.007.

[47] N. Diamanti and D. Redman, "Field observations and numerical models of GPR response from vertical pavement cracks," *J. Appl. Geophys.*, vol. 81, pp. 106–116, 2012, doi: 10.1016/j.jappgeo.2011.09.006.

[48] F. M. Fernandes, A. Fernandes, and J. Pais, "Assessment of the density and moisture content of asphalt mixtures of road pavements," *Constr. Build. Mater.*, vol. 154, pp. 1216–1225, 2017, doi: 10.1016/j.conbuildmat.2017.06.119.

[49] Rasol, M. A., Pérez-Gracia, V., Fernandes, F. M., Pais, J. C., Santos-Assunçao, S., Santos, C., & Sossa, V. (2020). GPR laboratory tests and numerical models to characterize cracks in cement concrete specimens, exemplifying damage in rigid pavement. *Measurement*, *158*, 107662.

[50] M. Solla, S. Lagüela, H. González-Jorge, and P. Arias, "Approach to identify cracking in asphalt pavement using GPR and infrared thermographic methods: Preliminary findings," *NDT E Int.*, vol. 62, pp. 55–65, 2014, doi: 10.1016/j.ndteint.2013.11.006.

[51] J. Pedret Rodés, V. Pérez-Gracia, and A. Martínez-Reguero, "Evaluation of the GPR frequency spectra in asphalt pavement assessment," *Constr. Build. Mater.*, vol. 96, pp. 181–188, 2015, doi: 10.1016/j.conbuildmat.2015.08.017.

[52] L. Krysiński and J. Sudyka, "GPR abilities in investigation of the pavement transversal cracks," *J. Appl. Geophys.*, vol. 97, pp. 27–36, 2013, doi: 10.1016/j.jappgeo.2013.03.010.

[53] Y. Jin and Y. Duan, "2D Wavelet Decomposition and F-K Migration for Identifying Fractured Rock Areas Using Ground Penetrating Radar," *Remote Sens.*, vol. 13, no. 12, p. 2280, 2021, doi: 10.3390/rs13122280.

[54] S. Fontul, "Strutural Evaluation of Flexible Pavements Using Non-Destrutive Tests," Ph.D Thesis, University of Coimbra. http://hdl.handle.net/10316/15738 November, 2004.

[55] M. Heitzman *et al.*, *Nondestructive Testing to Identify Delaminations Between HMA Layers, Volume 1 - Summary*, vol. 1. 2013.

[56] S. S. Todkar, C. Le Bastard, V. Baltazart, A. Ihamouten, and X. Dérobert, "Performance assessment of SVM-based classification techniques for the detection of artificial debondings within pavement structures from stepped-frequency A-scan radar data," *NDT E Int.*, vol. 107, no. June, p. 102128, 2019, doi: 10.1016/j.ndteint.2019.102128.

[57] X. Dérobert, V. Baltazart, J. M. Simonin, S. S. Todkar, C. Norgeot, and H. Y. Hui, "GPR monitoring of artificial debonded pavement structures throughout its life cycle during accelerated pavement testing," *Remote Sens.*, vol. 13, no. 8, 2021, doi: 10.3390/rs13081474.

[58] J.-M. Simonin, V. Baltazart, C. Le Bastard, and X. Dérobert, "Progress in Monitoring the Debonding Within Pavement Structures During Accelerated Pavement Testing on the Fatigue Carousel," in *8th RILEM International Conference on Mechanisms of Cracking and Debonding in Pavements*, 2016, pp. 749–755.

[59] ASTM D4580-86, "Standard Practice for Measuring Delaminations in Concrete Bridge Decks by Sounding," 1992.

[60] ASTM D6429-20, "Standard Guide for Selecting Surface Geophysical Methods," Philadelphia, PA, 1999.

[61] Ó. P. Anchuela, A. M. Casas-Sainz, A. Pocoví-Juan, H. G. Garbí, and P. Calvín, "Characterization of the Karstic Process in an Urban Environment Using GPR Surveys," *J. Mater. Civ. Eng.*, vol. 26, no. 8, p. 05014004, 2014, doi: 10.1061/(asce)mt.1943-5533.0001072.

[62] S. Tomecka-Suchoń and H. Marcak, "Interpretation of Ground Penetrating Radar Attributes in Identifying the Risk of Mining Subsidence," *Arch. Min. Sci.*, vol. 60, no. 2, pp. 645–656, 2015, doi: 10.1515/amsc-2015-0042.

[63] T. Thitimakorn, N. Kampananon, N. Jongjaiwanichkit, and S. Kupongsak, "Subsurface void detection under the road surface using ground penetrating radar (GPR), a case study in the Bangkok metropolitan area, Thailand," *Int. J. Geo-Engineering*, vol. 7, no. 1, 2016, doi: 10.1186/s40703-016-0017-8.

[64] W. T. Hong, S. Kang, S. J. Lee, and J. S. Lee, "Analyses of GPR signals for characterization of ground conditions in urban areas," *J. Appl. Geophys.*, vol. 152, pp. 65–76, 2018, doi: 10.1016/j.jappgeo.2018.03.005.

[65] S. Lagüela, M. Solla, I. Puente, and F. J. Prego, "Joint use of GPR, IRT and TLS techniques for the integral damage detection in paving," *Constr. Build. Mater.*, vol. 174, pp. 749–760, 2018, doi:

10.1016/j.conbuildmat.2018.04.159.
[66] A. K. Pandey, J. Gogoi, and P. Pandey, “Mapping shallow subsurface to identify sinkhole formation in urban areas using ground penetration radar: A case study from Hyderabad, India,” *Curr. Sci.*, vol. 117, no. 10, pp. 1710–1715, 2019, doi: 10.18520/cs/v117/i10/1710-1715.
[67] A. Ronen, M. Ezersky, A. Beck, B. Gatenio, and R. B. Simhayov, “Use of GPR method for prediction of sinkholes formation along the Dead Sea Shores, Israel,” *Geomorphology*, vol. 328, pp. 28–43, 2019, doi: 10.1016/j.geomorph.2018.11.030.
[68] L. Capozzoli, G. De Martino, M. Polemio, and E. Rizzo, “Geophysical Techniques for Monitoring Settlement Phenomena Occurring in Reinforced Concrete Buildings,” *Surv. Geophys.*, vol. 41, no. 3, pp. 575–604, 2019, doi: 10.1007/s10712-019-09554-8.
[69] J. Sevil *et al.*, “Characterizing and monitoring a high-risk sinkhole in an urban area underlain by salt through non-invasive methods: Detailed mapping, high-precision leveling and GPR,” *Eng. Geol.*, vol. 272, no. April, p. 105641, 2020, doi: 10.1016/j.enggeo.2020.105641.
[70] S. Liu, Q. Lu, H. Li, and Y. Wang, “Estimation of moisture content in railway subgrade by ground penetrating radar,” *Remote Sens.*, vol. 12, no. 18, pp. 1–15, 2020, doi: 10.3390/RS12182912.
[71] G. C. Topp, J. L. Davis, and A. P. Annan, “Electromagnetic determination of soil water content: Measurements in coaxial transmission lines,” *Water Resour. Res.*, vol. 16, no. 3, pp. 574–582, 1980, doi: 10.1029/WR016i003p00574.
[72] I. Al-Qadi, S. Lahouar, A. Loulizi, M. A. Elseifi, and J. A. Wilkes, “Effective approach to improve pavement drainage layers,” *J. Transp. Eng.*, vol. 130, no. 5, pp. 658–664, 2004, doi: 10.1061/(ASCE)0733-947X(2004)130:5(658).
[73] K. R. Maser and T. Scullion, “Automated Pavement Subsurface Profiling Using Radar: Case Studies of Four Experimental Field Sites,” *Transp. Res. Rec.*, vol. 1344, pp. 148–154, 1992, [Online]. Available: https://trid.trb.org/view/370805.
[74] A. A. M. Venmans, R. Van De Ven, and J. Kollen, “Rapid and Non-intrusive Measurements of Moisture in Road Constructions Using Passive Microwave Radiometry and GPR - Full Scale Test,” *Procedia Eng.*, vol. 143, no. Ictg, pp. 1244–1251, 2016, doi: 10.1016/j.proeng.2016.06.111.
[75] C. Berthelot, D. Podborochynski, T. Saarenketo, B. Marjerison, and C. Prang, “Ground-penetrating radar evaluation of moisture and frost across typical Saskatchewan road soils,” *Adv. Civ. Eng.*, vol. 2010, 2010, doi: 10.1155/2010/416190.
[76] J. Zhang *et al.*, “In-situ recognition of moisture damage in bridge deck asphalt pavement with time-frequency features of GPR signal,” *Constr. Build. Mater.*, vol. 244, p. 118295, 2020, doi: 10.1016/j.conbuildmat.2020.118295.
[77] J. Zhang, X. Yang, W. Li, S. Zhang, and Y. Jia, “Automatic detection of moisture damages in asphalt pavements from GPR data with deep CNN and IRS method,” *Autom. Constr.*, vol. 113, no. September 2019, p. 103119, 2020, doi: 10.1016/j.autcon.2020.103119.
[78] A. M. St. Clair and S. Sinha, “State-of-the-technology review on water pipe condition, deterioration and failure rate prediction models!,” *Urban Water J.*, vol. 9, no. 2, pp. 85–112, 2012, doi: 10.1080/1573062X.2011.644566.
[79] M. J. Anbari, M. Tabesh, and A. Roozbahani, “Risk assessment model to prioritize sewer pipes inspection in wastewater collection networks,” *J. Environ. Manage.*, vol. 190, pp. 91–101, 2017, doi: 10.1016/j.jenvman.2016.12.052.
[80] A. Akbarpour, S. Chamaani, J. Sachs, and G. Del Galdo, “Clutter Removal of Near-Field UWB SAR Imaging for Pipeline Penetrating Radar,” *IEEE J. Sel. Top. Appl. Earth Obs. Remote Sens.*, vol. 13, pp. 1527–1539, 2020, doi: 10.1109/JSTARS.2020.2983891.
[81] Z. Liu and Y. Kleiner, “State of the art review of inspection technologies for condition assessment of water pipes,” *Meas. J. Int. Meas. Confed.*, vol. 46, no. 1, pp. 1–15, 2013, doi: 10.1016/j.measurement.2012.05.032.
[82] S. Zhao and I. Al-Qadi, “Pavement drainage pipe condition assessment by GPR image reconstruction using FDTD modeling,” *Constr. Build. Mater.*, vol. 154, pp. 1283–1293, 2017, doi: 10.1016/j.conbuildmat.2017.06.103.
[83] C. Ékes, B. Neducza, G. R. Henrich, and S. T. Corp, “Gpr Goes Underground : Pipe Penetrating Radar,” pp. 1–10, 2011.
[84] D. A. Cabrera, “Characterization of components of water supply systems from {GPR} images and tools of intelligent data analysis.,” no. December, 2015, [Online]. Available: https://riunet.upv.es/handle/10251/59235.
[85] D. Ayala-Cabrera, S. J. Ocana-Levario, J. Izquierdo, and R. Perez-Garcia, “3D Representation of (Buried) Water Supply Elements using Pre-Processed GPR Images,” *Athens J. Technology Eng.*, vol. 3, no. 3, pp. 241–254, 2016, doi: 10.30958/ajte.3-3-3.
[86] F. B. Figueroa *et al.*, “Georadar y realidad aumentada : una aproximación a la visualización automática del trazado y las características de las tuberías en los sistemas de abastecimiento de agua,” no. November 2016, 2013.
[87] D. Ayala-Cabrera, E. Campbell, E. P. Carreño-Alvarado, J. Izquierdo, and R. Pérez-García, “Water Leakage

Evolution Based on GPR Interpretations," *Procedia Eng.*, vol. 89, pp. 304–310, 2014, doi: 10.1016/j.proeng.2014.11.192.

[88] T. Koganti, E. Ghane, L. R. Martinez, B. V. Iversen, and B. J. Allred, *Mapping of agricultural subsurface drainage systems using unmanned aerial vehicle imagery and ground penetrating radar*, vol. 21, no. 8. 2021.

[89] N. Šarlah, T. Podobnikar, T. Ambrožič, and B. Mušič, "Application of kinematic GPR-tps model with high 3d georeference accuracy for underground utility infrastructure mapping: A case study from urban sites in Celje, Slovenia," *Remote Sens.*, vol. 12, no. 8, 2020, doi: 10.3390/RS12081228.

[90] M. Gabryś and L. Ortyl, "Georeferencing of multi-channel GPR-accuracy and efficiency of mapping of underground utility networks," *Remote Sens.*, vol. 12, no. 18, 2020, doi: 10.3390/RS12182945.

[91] V. Donazzolo and R. Yelf, "Determination of wall thickness and condition of Asbestos Cement pipes in sewer rising mains using Surface Penetrating Radar," *Proc. 13th Internarional Conf. Gr. Penetrating Radar, GPR 2010*, pp. 1–5, 2010, doi: 10.1109/ICGPR.2010.5550183.

[92] R. N. Deo, R. M. Azoor, and J. K. Kodikara, "Proof of concept using numerical simulations for pipe corrosion inferences using ground penetrating radar," *2017 9th Int. Work. Adv. Gr. Penetrating Radar, IWAGPR 2017 - Proc.*, pp. 1–5, 2017, doi: 10.1109/IWAGPR.2017.7996092.

[93] H. Noshahri, L. O. Scholtenhuis M. Van Delft, J. F. Hempenius, and E. Dertien, "Towards Underground Void Detection with In-pipe Ground Penetrating Radar," vol. 2020, no. 1, pp. 1–5, 2020, doi: https://doi.org/10.3997/2214-4609.202071025.

[94] F. Garcia-Garcia, A. Valls-Ayuso, J. Benlloch-Marco, and M. Valcuende-Paya, "An optimization of the work disruption by 3D cavity mapping using GPR: A new sewerage project in Torrente (Valencia, Spain)," *Constr. Build. Mater.*, vol. 154, pp. 1226–1233, 2017, doi: 10.1016/j.conbuildmat.2017.06.116.

[95] D. H. Koo and S. T. Ariaratnam, "Innovative method for assessment of underground sewer pipe condition," *Autom. Constr.*, vol. 15, no. 4, pp. 479–488, 2006, doi: 10.1016/j.autcon.2005.06.007.

[96] C. Ekes and Boriszlav Neducza, "Pipe condition assessments using Pipe Penetrating Radar," in *2012 14th International Conference on Ground Penetrating Radar (GPR)*, 2012, pp. 840–843.

[97] D. Ayala-Cabrera and J. Izquierdo, "GPR image interpretation advancement for smarter technical management of water leakage in urban water infrastructures," in *Earth Resources and Environmental Remote Sensing/GIS Applications XII*, 2021, vol. 11863, pp. 220–227, doi: 10.1117/12.2599943.

[98] S. Demirci, E. Yigit, I. H. Eskidemir, and C. Ozdemir, "Ground penetrating radar imaging of water leaks from buried pipes based on back-projection method," *NDT E Int.*, vol. 47, pp. 35–42, 2012, doi: 10.1016/j.ndteint.2011.12.008.

[99] M. Pitoňák and J. Filipovsky, "GPR Application - Non-destructive Technology for Verification of Thicknesses of Newly Paved Roads in Slovakia," *Procedia Eng.*, vol. 153, pp. 537–549, 2016, doi: 10.1016/j.proeng.2016.08.184.

[100] T. Scullion and T. Saarenketo, "STP1375-Integrating Ground Penetrating Radar and Falling Weight Deflectometer Technologies in Pavement Evaluation," *Nondestruct. Test. Pavements Backcalc. Modul. Third Vol. ed. S. Tayabji E. Lukanen (West Conshohocken, PA ASTM Int. 2000)*, pp. 23–37, 2000, [Online]. Available: https://doi.org/10.1520/STP14758S.

[101] J. Domitrović and T. Rukavina, "Application of GPR and FWD in Assessing Pavement Bearing Capacity," *Rom. J. Transp. Infrastruct.*, vol. 2, no. 2, pp. 11–21, 2013, doi: 10.1515/rjti-2015-0015.

[102] C. Plati, A. Loizos, and K. Gkyrtis, "Integration of non-destructive testing methods to assess asphalt pavement thickness," *NDT E Int.*, vol. 115, no. May, p. 102292, 2020, doi: 10.1016/j.ndteint.2020.102292.

[103] W. Muller, "A comparison of TSD, FWD and GPR field measurements," *Int. Symp. Non-Destructive Test. Civ. Eng.*, no. November, p. 10, 2015.

[104] K. Maser, P. Schmalzer, W. Shaw, and A. Carmichael, "Integration of traffic speed deflectometer and ground-penetrating radar for network-level roadway structure evaluation," *Transp. Res. Rec.*, vol. 2639, no. 1, pp. 55–63, 2017, doi: 10.3141/2639-08.

[105] M. Varela-González, M. Solla, J. Martínez-Sánchez, and P. Arias, "A semi-automatic processing and visualisation tool for ground-penetrating radar pavement thickness data," *Autom. Constr.*, vol. 45, no. March 2018, pp. 42–49, 2014, doi: 10.1016/j.autcon.2014.05.004.

[106] D. Carbonel *et al.*, "Investigating a damaging buried sinkhole cluster in an urban area (Zaragoza city, NE Spain) integrating multiple techniques: Geomorphological surveys, DInSAR, DEMs, GPR, ERT, and trenching," *Geomorphology*, 2015, doi: 10.1016/j.geomorph.2014.02.007.

[107] M. C. Diallo, L. Z. Cheng, E. Rosa, C. Gunther, and M. Chouteau, "Integrated GPR and ERT data interpretation for bedrock identification at Cléricy, Québec, Canada," *Eng. Geol.*, vol. 248, no. January 2018, pp. 230–241, 2019, doi: 10.1016/j.enggeo.2018.09.011.

[108] L. Nuzzo, G. Leucci, and S. Negri, "GPR, VES and refraction seismic surveys in the karstic area 'Spedicaturo' near Nociglia (Lecce, Italy)," *Near Surf. Geophys.*, vol. 5, no. 1, pp. 67–76, 2007, doi: 10.3997/1873-0604.2006019.

[109] L. De Giorgi and G. Leucci, "Detection of Hazardous Cavities Below a Road Using Combined Geophysical Methods," *Surv. Geophys.*, vol. 35, no. 4, pp. 1003–1021, 2014, doi: 10.1007/s10712-013-9277-4.

[110] L. B. Ciampoli, V. Gagliardi, C. Ferrante, A. Calvi, F. D'amico, and F. Tosti, "Displacement monitoring in

airport runways by persistent scatterers sar interferometry," *Remote Sens.*, vol. 12, no. 21, pp. 1–14, 2020, doi: 10.3390/rs12213564.

[111] R. Martel, P. Castellazzi, E. Gloaguen, L. Trépanier, and J. Garfias, "ERT, GPR, InSAR, and tracer tests to characterize karst aquifer systems under urban areas: The case of Quebec City," *Geomorphology*, vol. 310, pp. 45–56, 2018, doi: 10.1016/j.geomorph.2018.03.003.

[112] A. Busetti, C. Calligaris, E. Forte, G. Areggi, A. Mocnik, and L. Zini, "Non-invasive methodological approach to detect and characterize high-risk sinkholes in urban cover evaporite karst: Integrated reflection seismics, PS-INSAR, leveling, 3D-GPR and ancillary data. a Ne Italian case study," *Remote Sens.*, vol. 12, no. 22, pp. 1–28, 2020, doi: 10.3390/rs12223814.

[113] H. Sun, S. Pashoutani, and J. Zhu, "Nondestructive evaluation of concrete bridge decks with automated acoustic scanning system and ground penetrating radar," *Sensors (Switzerland)*, vol. 18, no. 6, 2018, doi: 10.3390/s18061955.

[114] S. Abu Dabous, S. Yaghi, S. Alkass, and O. Moselhi, "Concrete bridge deck condition assessment using IR Thermography and Ground Penetrating Radar technologies," *Autom. Constr.*, vol. 81, no. April, pp. 340–354, 2017, doi: 10.1016/j.autcon.2017.04.006.

[115] A. V. Varnavina, L. H. Sneed, A. K. Khamzin, E. V. Torgashov, and N. L. Anderson, "An attempt to describe a relationship between concrete deterioration quantities and bridge deck condition assessment techniques," *J. Appl. Geophys.*, vol. 142, pp. 38–48, 2017, doi: 10.1016/j.jappgeo.2017.05.009.

[116] N. J. Cassidy, R. Eddies, and S. Dods, "Void detection beneath reinforced concrete sections: The practical application of ground-penetrating radar and ultrasonic techniques," *J. Appl. Geophys.*, vol. 74, no. 4, pp. 263–276, 2011, doi: 10.1016/j.jappgeo.2011.06.003.

[117] M. Abouhamad, T. Dawood, A. Jabri, M. Alsharqawi, and T. Zayed, "Corrosiveness mapping of bridge decks using image-based analysis of GPR data," *Autom. Constr.*, vol. 80, pp. 104–117, 2017, doi: 10.1016/j.autcon.2017.03.004.

[118] K. Dinh, N. Gucunski, and T. Zayed, "Automated visualization of concrete bridge deck condition from GPR data," *NDT E Int.*, vol. 102, no. November 2018, pp. 120–128, 2019, doi: 10.1016/j.ndteint.2018.11.015.

[119] Z. Zong *et al.*, "A deep learning approach for urban underground objects detection from vehicle-borne ground penetrating radar data in real-time," *Int. Arch. Photogramm. Remote Sens. Spat. Inf. Sci. - ISPRS Arch.*, vol. 42, no. 2/W16, pp. 293–299, 2019, doi: 10.5194/isprs-archives-XLII-2-W16-293-2019.

[120] N. Kim, K. Kim, Y. K. An, H. J. Lee, and J. J. Lee, "Deep learning-based underground object detection for urban road pavement," *Int. J. Pavement Eng.*, vol. 21, no. 13, pp. 1638–1650, 2020, doi: 10.1080/10298436.2018.1559317.

[121] F. Ponti *et al.*, "GPR radargrams analysis through machine learning approach," *J. Electromagn. Waves Appl.*, vol. 35, no. 12, pp. 1678–1686, 2021, doi: 10.1080/09205071.2021.1906329.

[122] W. Al-Nuaimy, Y. Huang, M. Nakhkash, M. T. C. Fang, V. T. Nguyen, and A. Eriksen, "Automatic detection of buried utilities and solid objects with GPR using neural networks and pattern recognition," *J. Appl. Geophys.*, vol. 43, no. 2–4, pp. 157–165, 2000, doi: 10.1016/S0926-9851(99)00055-5.

[123] W. Lei, J. Luo, F. Hou, L. Xu, R. Wang, and X. Jiang, "Underground cylindrical objects detection and diameter identification in GPR B-scans via the CNN-LSTM framework," *Electron.*, vol. 9, no. 11, pp. 1–16, 2020, doi: 10.3390/electronics9111804.

[124] D. Kumlu and B. Gundogdu, "A Novel Tensor RPCA Method for Clutter Suppression in GPR Images," no. April, 2021.

[125] M. Kang and Y. An, "Frequency–Wavenumber Analysis of Deep Learning-based Super Resolution 3D GPR Images," 2020.

[126] M. S. Kang, N. Kim, S. B. Im, J. J. Lee, and Y. K. An, "3D GPR image-based UcNet for enhancing underground cavity detectability," *Remote Sens.*, vol. 11, no. 21, pp. 1–18, 2019, doi: 10.3390/rs11212545.

[127] M. S. Kang, N. Kim, J. J. Lee, and Y. K. An, "Deep learning-based automated underground cavity detection using three-dimensional ground penetrating radar," *Struct. Heal. Monit.*, vol. 19, no. 1, pp. 173–185, 2020, doi: 10.1177/1475921719838081.

[128] M. T. Pham and S. Lefèvre, "Buried object detection from B-scan ground penetrating radar data using Faster-RCNN," *Int. Geosci. Remote Sens. Symp.*, vol. 2018-July, pp. 6804–6807, 2018, doi: 10.1109/IGARSS.2018.8517683.

[129] J. Zhang, X. Yang, W. Li, S. Zhang, and Y. Jia, "Automatic detection of moisture damages in asphalt pavements from GPR data with deep CNN and IRS method," *Autom. Constr.*, vol. 113, no. February, p. 103119, 2020, doi: 10.1016/j.autcon.2020.103119.

[130] Y. Jin and Y. Duan, "Wavelet scattering network-based machine learning for ground penetrating radar imaging: Application in pipeline identification," *Remote Sens.*, vol. 12, no. 21, pp. 1–24, 2020, doi: 10.3390/rs12213655.

[131] S. Li *et al.*, "Detection of concealed cracks from ground penetrating radar images based on deep learning algorithm," *Constr. Build. Mater.*, vol. 273, p. 121949, 2021, doi: 10.1016/j.conbuildmat.2020.121949.

[132] J. Gao, D. Yuan, Z. Tong, J. Yang, and D. Yu, "Autonomous pavement distress detection using ground penetrating radar and region-based deep learning," *Meas. J. Int. Meas. Confed.*, vol. 164, 2020, doi:

10.1016/j.measurement.2020.108077.
[133] C. Le Bastard, V. Baltazart, X. Dérobert, and Y. Wang, "Support vector regression method applied to thin pavement thickness estimation by GPR," *2012 14th Int. Conf. Gr. Penetrating Radar, GPR 2012*, no. 2, pp. 349–353, 2012, doi: 10.1109/icgpr.2012.6254888.
[134] X. Bai, W. An, B. Wang, J. Jiang, Y. Zhang, and J. Zhang, "Automatic Identification of Underground Pipeline Based on Ground Penetrating Radar," in *Wireless and Satellite Systems*, 2019, pp. 70–78.
[135] C. Liu, Y. Zhan, Q. Deng, Y. Qiu, and A. Zhang, "An improved differential box counting method to measure fractal dimensions for pavement surface skid resistance evaluation," *Measurement*, vol. 178, no. January, p. 109376, 2021, doi: 10.1016/j.measurement.2021.109376.
[136] X. Zhang, L. Han, M. Robinson, and A. Gallagher, "A Gans-Based Deep Learning Framework for Automatic Subsurface Object Recognition from Ground Penetrating Radar Data," *IEEE Access*, vol. 9, pp. 39009–39018, 2021, doi: 10.1109/ACCESS.2021.3064205.
[137] M. Rith, Y. K. Kim, and S. W. Lee, "Characterization of long-term skid resistance in exposed aggregate concrete pavement," *Constr. Build. Mater.*, vol. 256, p. 119423, 2020, doi: 10.1016/j.conbuildmat.2020.119423.
[138] X. Dérobert and L. Pajewski, "TU1208 Open Database of Radargrams: The Dataset of the IFSTTAR Geophysical Test Site," *Remote Sens.*, vol. 10, no. 4, p. 530, 2018, doi: 10.3390/rs10040530.
[139] I. X. Chen, "irenexychen/gpr-data-classifier." Accessed August 06, 2021. https://github.com/irenexychen/gpr-data-classifier," 2021. .
[140] C. Warren, A. Giannopoulos, and I. Giannakis, "gprMax: Open source software to simulate electromagnetic wave propagation for Ground Penetrating Radar," *Comput. Phys. Commun.*, 2016, doi: 10.1016/j.cpc.2016.08.020.
[141] C. Warren *et al.*, "A CUDA-based GPU engine for gprMax: Open source FDTD electromagnetic simulation software," *Comput. Phys. Commun.*, Nov. 2018, doi: 10.1016/J.CPC.2018.11.007.
[142] D. Ayala-Cabrera, J. Izquierdo, I. Montalvo, and R. Pérez-García, "Water supply system component evaluation from GPR radargrams using a multi-agent approach," *Math. Comput. Model.*, vol. 57, no. 7–8, pp. 1927–1932, 2013, doi: 10.1016/j.mcm.2011.12.034.
[143] D. Ayala-Cabrera, M. Herrera, J. Izquierdo, and R. Pérez-García, "Location of buried plastic pipes using multi-agent support based on GPR images," *J. Appl. Geophys.*, 2011, doi: 10.1016/j.jappgeo.2011.09.024.
[144] B. Zhang *et al.*, "A BP Neural Network Method for Grade Classification of Loose Damage in Semirigid Pavement Bases," *Adv. Civ. Eng.*, vol. 2021, 2021, doi: 10.1155/2021/6658235.
[145] H. Manico, "Characterization and application of BIM methodologies. MsC dissertation. Nova University of Lisbon, Portugal (in Portuguese, 2018).," 2018.
[146] S. Fontul, "Future Trends in Transport Infrastructure Monitoring," no. October, pp. 261–265, 2019, doi: 10.5592/co/ftce.2019.12.
[147] S. A. Biancardo, N. Viscione, C. Oreto, R. Veropalumbo, and F. Abbondati, "BIM approach for modeling airports terminal expansion," *Infrastructures*, vol. 5, no. 5, pp. 1–14, 2020, doi: 10.3390/infrastructures5050041.
[148] S. Karimzadeh and M. Matsuoka, "Remote sensing x-band sar data for land subsidence and pavement monitoring," *Sensors (Switzerland)*, vol. 20, no. 17, pp. 1–21, 2020, doi: 10.3390/s20174751.
[149] N. Fiorentini, M. Maboudi, P. Leandri, M. Losa, and M. Gerke, "Surface motion prediction and mapping for road infrastructures management by PS-InSAR measurements and machine learning algorithms," *Remote Sens.*, vol. 12, no. 23, pp. 1–60, 2020, doi: 10.3390/rs12233976.
[150] D. Goulias and M. L. Scott, "Effective Implementation of Ground Penetrating Radar (GPR) for Condition Assessment & Monitoring of Critical Infrastructure Components of Bridges and Highways," p. 183, 2015.
[151] S. Carpitella, S. J. Ocaña-Levario, J. Benítez, A. Certa, and J. Izquierdo, "A hybrid multi-criteria approach to GPR image mining applied to water supply system maintenance," *J. Appl. Geophys.*, vol. 159, pp. 754–764, 2018, doi: 10.1016/j.jappgeo.2018.10.021.

Graphical Abstract

GPR Monitoring for Road Transport Infrastructure: A Systematic Review and Machine Learning Insights

1 Principles of GPR, and objectives of the study

GPR principles

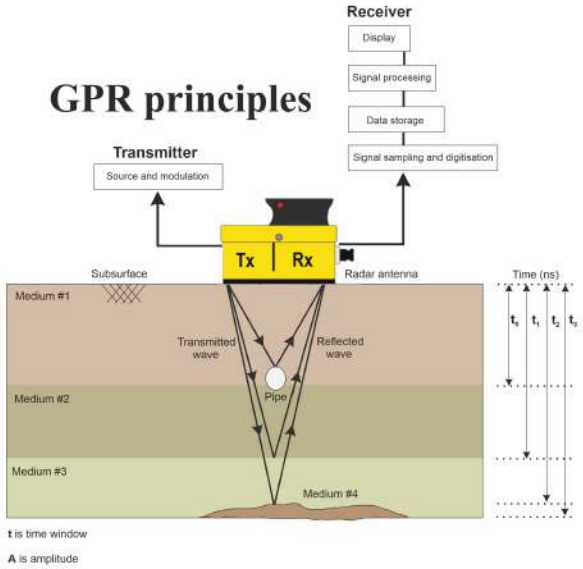

Research gaps vs contribution

Current research gaps	Main brief contribution of study
1. Lack of possible review study to understand main distresses in road pavements, and the efficiency of GPR in the monitoring process.	1. comprehnsively review of diverse distressed in road pavement, and illustrating the capacity of GPR, which can be a useful source for road engineers, and researchers in road pavement monitoring.
2. The main intelligent data analysis approaches which can be efficient for enhancing radarimages interoperability, and provide significant decision-making tools for road transport owners, or operators.	2. State-of-the-art of the machine learning based approaches are presented, and this could support researchers are working on developing decision-making tools, and enhnace a better interprobility of radar images

2 Road transport distresses

Settlement and filling subsidence

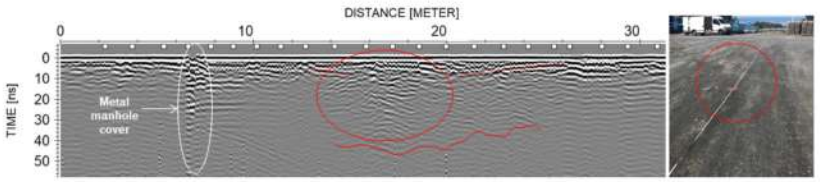

Discontinuities in between layer thicknesses

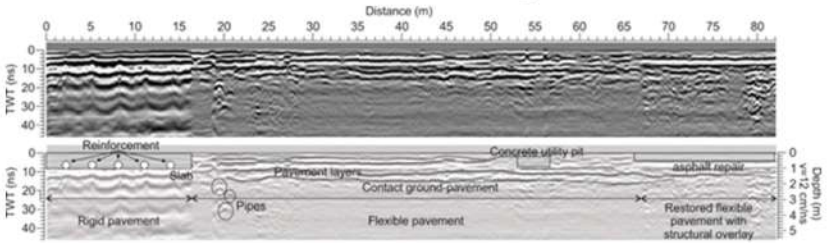

3 Incorporation of other NDTs with GPR and Intelligent data analysis

Incorporation of NDTs with GPR

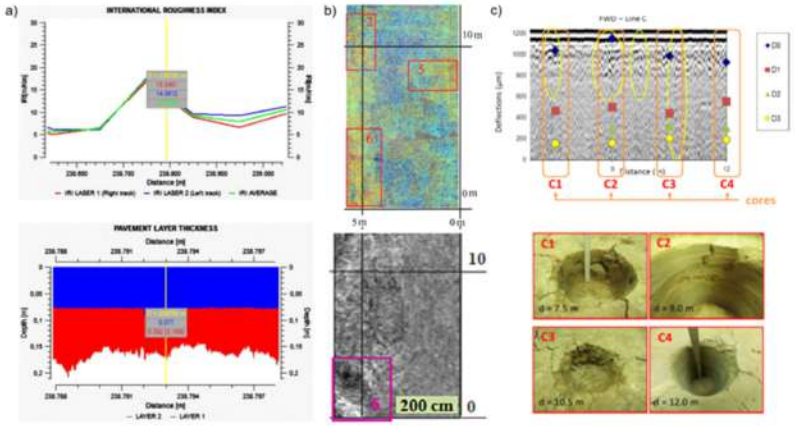

Machine learning based approaches